

**The Effects of Orciprenaline on the Contractility of  
Isolated Cardiomyocytes under Septic Conditions  
Mediated by Lipopolysaccharide**

Inaugural-Dissertation  
zur Erlangung des Doktorgrades  
der Hohen Medizinischen Fakultät  
der Rheinischen Friedrich-Wilhelms-Universität  
Bonn

**Joon Young Seo**

aus Seoul/Korea

2018

Angefertigt mit der Genehmigung  
der Medizinischen Fakultät der Universität Bonn

1. Gutachter: Prof. Dr. rer. nat. Rainer Meyer
2. Gutachter: Prof. Dr. med. Michael Hölzel

Tag der Mündlichen Prüfung: 22.05.2018

This work has been carried out in the Institute of Physiology, University of Bonn  
Director: Prof. Dr. med. Dieter Swandulla

Meiner Woo Youn



## Table of Contents

<b>List of Abbreviations</b> .....	8
<b>1 Introduction</b> .....	10
1.1 History and Epidemiology of Sepsis.....	10
1.2 The structure and the Function of the Cardiomyocyte.....	12
1.3 Pathogenesis of the Reduction of Myocardial Contractility.....	13
1.4 Objective of this Study.....	17
<b>2 Material and Method</b> .....	18
2.1 Test Animals and Maintenance Conditions.....	18
2.2 Description of the Experimental Method and Cell Groups.....	18
2.2.1 Isolation of Ventricular Cardiomyocytes.....	19
2.2.2 Incubation of the Isolated Cells.....	24
2.2.2.1 The Culture Medium.....	25
2.2.2.2 Lipopolysaccharide.....	25
2.2.3 Measurement of Sarcomere Shortening.....	25
2.2.3.1 Experimental Set Up.....	25
2.2.3.2 Test Chamber.....	27
2.2.3.3 Coating of the Measuring Area with the Cardiomyocytes.....	28
2.2.3.4 The Perfusion System.....	29
2.2.3.5 The External, Electrical Stimulation.....	29
2.2.3.6 $\beta$ -Stimulation with Orciprenaline.....	30
2.2.4 The Principle of the optical Sarcomere Length Measurement.....	31
2.3 Data Acquisition and Analysis.....	32
2.3.1 Analysis of the Data Set Acquired during the Sarcomere Shortening.....	32
2.3.2 Statistics.....	36
<b>3 Results</b> .....	37
3.1 The Number of Test Animals used.....	37
3.2 Cell Groups.....	37
3.3 Original Registrations.....	38
3.4 Contraction Parameters.....	43
3.4.1 Resting Sarcomere Length, Tyrode vs. Tyrode + Orciprenaline.....	43

3.4.1.1	Resting Sarcomere Length, Tyrode vs. Culture Medium + Orciprenaline....	44
3.4.1.2	Resting Sarcomere Length, Culture Medium + LPS vs. Culture Medium + LPS + Orciprenaline.....	45
3.4.2	Sarcomere Shortening Amplitude, Tyrode vs. Tyrode + Orciprenaline.....	46
3.4.3	Sarcomere Shortening Speed, Tyrode vs. Tyrode + Orciprenaline.....	47
3.4.4	Sarcomere Relaxation Speed.....	48
3.4.4.1	Relaxation Speed, Tyrode vs. Tyrode + Orciprenaline.....	49
3.4.5	Sarcomere Shortening Amplitude in Culture Medium.....	50
3.4.5.1	Sarcomere Shortening Amplitude, Tyrode + Orciprenaline vs. Culture Medium + Orciprenaline.....	51
3.4.6	Sarcomere Shortening Speed, Culture Medium + Orciprenaline vs. Tyrode vs. Culture Medium.....	52
3.4.7	Relaxation Speed, Tyrode vs. Culture Medium vs. Culture Medium + Orciprenaline.....	53
3.4.8	Sarcomere Shortening Amplitude, Culture Medium vs. Culture Medium + LPS vs. Culture Medium + LPS + Orciprenaline.....	54
3.4.9	Sarcomere Shortening Amplitude, Culture Medium + Orciprenaline vs. Culture Medium + LPS + Orciprenaline.....	55
3.4.10	Sarcomere Shortening Speed, Culture Medium vs. Culture Medium + LPS vs. Culture Medium + LPS + Orciprenaline.....	56
3.4.11	Sarcomere Shortening Speed, Culture Medium + Orciprenaline vs. Culture Medium + LPS + Orciprenaline.....	57
3.4.12	Sarcomere Relaxation Speed, Culture Medium vs. Culture Medium + LPS vs. Culture Medium + LPS + Orciprenaline.....	58
<b>4</b>	<b>Discussion</b> .....	<b>59</b>
4.1	Validity of the Method.....	59
4.2	The effects of orciprenaline on the shortening of cardiomyocytes.....	61
4.3	Signal Cascade from TLR4 to Cardiac Depression in the Presence of Lipopolysaccharide.....	62
4.4	“Rescue Effect” of Orciprenaline in the Presence of LPS.....	63
4.5	Conclusion.....	66
<b>5</b>	<b>Zusammenfassung</b> .....	<b>66</b>

<b>6</b>	<b>References</b> .....	<b>67</b>
<b>7</b>	<b>Supplement: Tables of Measured Parameters</b> .....	<b>76</b>
7.1	Legend.....	76
7.2	Resting Sarcomere Length.....	77
7.3	Shortening Amplitude.....	78
7.4	Shortening Speed.....	79
7.5	Relaxation Speed.....	80
<b>8</b>	<b>Acknowledgements</b> .....	<b>81</b>

## List of Abbreviations

ACCP	American College of Chest Physicians
ATP	Adenosine Triphosphate
BSA	Bovine Serum Albumin
cAMP	Cyclic Adenosine Monophosphate
CD14	Cluster of Differentiation 14
CpG	Cytosin-Phosphate-Guanosin
CpG-ODN	CpG- Oligodesoxynucleotide
Ca <sup>+</sup>	Calcium Ion
CaCl <sub>2</sub>	Calcium Chloride
CO <sub>2</sub>	Carbondioxide
DD	Death domain of MyD88
DNA	Deoxyribonucleic Acid
EGTA	Ethylene Glycol Tetra Acetic Acid
h	Hour
HEPES	(4-(2-hydroxyethyl)-1-piperazineethanesulfonic acid
Hz	Hertz
IL-1 $\beta$	Interleukin 1 $\beta$
Inc.	Incorporated
iNOS	inducible Nitricoxide Synthase
IRAK	IL-1Receptor Associated Kinase
K <sup>+</sup>	Potassium Ion
KCl	Potassium Chloride
kDa	Kilodalton
KOH	Potassium Hydroxide
LPS	Lipopolysaccharide
M	Molar
MAPK	Mitogen Activated Protein Kinase
MgCl <sub>2</sub>	Magnesiumchloride
mg	Milligram
ml	Milliliter



mm	Millimeter
mmHg	Millimeter Mercury
mM	Millimolar
mMol	Millimol
μl	Microliter
μm	Micrometer
μMol	Micromol
mRNA	Messenger RNA
MODS	Multiple Organ Dysfunction Syndrome
ms	Millisecond
Aver.	Average
MyD88	Myeloid Differentiation Primary Response Gene 88
n	Number
NFκB	Nuclear Factor Kappa-light-chain-enhancer of Activated B Cells
Na <sup>+</sup>	Sodium Ion
NaCl	Sodium Chloride
NO	Nitric Oxide
O <sub>2</sub>	Oxygen Molecule
PAMP	Pathogen Associated Molecular Pattern
pH	Acid Dissociation Constant
Pro	Proline
PRRs	Pattern Recognition Receptors
SCCM	Society of Critical Care Medicine
SD	Standard Deviation
SEM	Standard Error of Mean
Ser	Serine
SIRS	Systemic Inflammatory Response Syndrome
SMT	S-methylisothiurea
TRAF6	TNF-Receptor Associated Factor 6
TNF-α	Tumor Necrosis Factor α
TLR	Toll-like-Receptor

# 1 Introduction

## 1.1 History and Epidemiology of Sepsis

Sepsis is a term describing a clinical condition in which a known or suspected pathogenic organism causes a potentially deadly whole body inflammation (Bone et al., 1992; Levy et al., 2003). It is also referred as "septicemia" or "blood poisoning". A septic patient usually has a focus of infection which spreads so rapidly that the body's own defense mechanisms cannot contain its progression to the whole body. A sepsis is frequently associated with several of the following unspecific symptoms: hyper- or hypothermia, leukocytosis or leucopenia, tachycardia and tachypnea.

While sepsis represents a major challenge in modern intensive medicine, it has been described often since ancient times. The renowned Greek physician Hippocrates (ca. 460 - 370 BC) already described sepsis with the Greek word σηπω (pronounced "sipsi") which means to "make rotten" (Kreymann, 1996). Ibn Sina (979-1037), an antique Persian physician, referred to sepsis as a sickness of the blood causing fever (Rittirsch et al., 2008). This rather vague concept was widely accepted in the western medicine until Ignaz Semmelweis (1818-1865) developed what was close to the modern view of sepsis. Semmelweis, an obstetrician at the Vienna General Hospital, observed that the high mortality rate of 18% at his department correlated to the frequency of pelvic examination on his patients performed by the medical students. These students examined the female patients directly after their pathology lessons without cleaning their hands. He concluded that the students must have caught "a decomposed animal matter that entered the blood system" which caused the deadly septic conditions in the patients (Semmelweis, 1861). He then introduced hand washing with a chlorinated lime solution before every gynecological examination and was able to reduce the mortality rate to about 2.5%. Semmelweis' observation shed some light on the understanding of septic infection. Furthermore, the discovery of bacteria by Louis Pasteur in 1857 helped scientists to understand the nature of an infection caused by bacterial pathogens (Pasteur, 1857). It was, however, not until the mass production of Penicillin after World War II that mankind could begin to fight against bacterial infection actively (Conly et al., 2005).

For the optimization of therapy strategies, a systematic understanding and a reliable classification of sepsis, a consensus conference between the American College of Chest Physicians (ACCP) and the Society of Critical Care Medicine (SCCM) was held in Chicago, IL in August, 1991 (ACCP/SCCM Consensus Conference Committee, 1992). There, a modern definition of sepsis and the guidelines for the use of innovative therapies in sepsis were developed for the purpose of “improving our ability to make early bedside detection of the disease possible, and thus allowing early therapeutic intervention” (Bone, 1992). The conference coined the term SIRS (Systemic Inflammatory Response Syndrome) and categorized sepsis into four levels (See Table 1).

Tab. 1: Definition of SIRS and sepsis (ACCP/SCCM-criteria)

SIRS (Systemic Inflammatory Response Syndrome)	Two or more of the following criteria (1) temperature >38°C or <36°C (2) heart rate >90 beats per minute (3) respiratory rate >20 breaths per minute or PaCO <sub>2</sub> , <32 mm Hg (4) white blood cell count >12,000 cells/μl, <4,000 cells/μl, or >10% immature (band) forms
Sepsis	Documented infection together with two or more SIRS criteria
Severe Sepsis	Sepsis associated with organ dysfunction, including, but not limited to, lactic acidosis, oliguria, hypoxemia, coagulation disorder, or an acute alteration in mental status.
Septic Shock	Sepsis with hypotension, despite adequate fluid resuscitation, along with the presence of perfusion abnormalities. Patients who are on inotropic or vasopressor agents may not be hypotensive at the time when perfusion abnormalities are detected.

In this classification, sepsis is differentiated from SIRS by the presence of a documented pathogen. For example, SIRS and a positive blood culture for a pathogen indicate the presence of a sepsis. In practice, however, in only about half of the suspected sepsis

cases the presence of a pathogen is actually verified through blood culture (Jones et al., 1996).

Today, there are at least 14 widely used types of antibacterial agents for humans by which a sepsis may be treated (Conly et al., 2005). Possibilities of device support for critical hemodynamic conditions in septic patients have been improving rapidly as well. Still, sepsis remains to be a major medical problem. In the United States sepsis is the second leading cause of death among non-cardiac Intensive Care Unit (ICU) patients, and the tenth most common cause of death overall, according to data from the Centers for Disease Control and Prevention (CDC, Martin et al., 2003). Sepsis is common and more hazardous for elderly, immune compromised and critically ill patients (Bone, 1992; Cohen, 2009). It occurs in 1–2% of all hospitalizations and accounts for as much as 25% of ICU bed utilization. The mortality rates range from 20% for sepsis, 40% for severe sepsis, to over 60% for septic shock.

## **1.2 The Structure and the Function of the Cardiomyocyte**

In observing the pathophysiological mechanism of a septic shock in an isolated cardiomyocyte, it is essential to have a clear understanding of the structure and the function of a cardiomyocyte. The cardiomyocyte belongs to the group of striated muscle cells that are connected together to form the myocardial tissue. Cardiomyocytes are about 50-100  $\mu\text{m}$  in length and have a single centrally positioned nucleus. Each cell is connected to one another in a branched manner through specialized sites known as intercalated discs (Franke et al., 2006). Two structures that are found within the intercalated discs are desmosomes and gap junctions. Desmosomes are specialized structures involved in cell-to-cell adhesion and gap junctions are intercellular channels that connect the cytoplasm of adjacent cells, allowing the free passage of molecules, ions and electrical signals. The most conspicuous structures in the cytoplasm of a cardiomyocyte are the myofibrils which enable the shortening of the cells. The myofibrils are responsible for the cross-striated appearance of the cardiomyocytes. Myofibrils are composed of sarcomeres which are the smallest contractile unit. Sarcomere length is around 1.8  $\mu\text{m}$  at rest (Craig et al., 2014). An increase of the cytoplasmic calcium ion concentration,  $[\text{Ca}^{2+}]_i$ , causes a shortening of the sarcomere, leading to myocardial

contraction. On the other hand, a decrease in  $[Ca^{2+}]_i$  induces relaxation of the myofilaments.

Electrical stimuli, called action potentials, AP, are required for cardiomyocyte contraction. The cardiac AP is initiated by a pacemaker located in the sinus node. The cardiac AP propagates across cardiomyocytes through gap junctions, allowing the cells to contract in a synchronized fashion, which enables the heart to contract as one muscle and thus to pump the blood in a coordinated manner (Craig et al., 2014).

An AP will depolarize the membrane potential and initiate a calcium inward current. This calcium inward current initiates a calcium release from the sarcoplasmic reticulum, which acts as the intracellular calcium store. As mentioned above, the increase in  $[Ca^{2+}]_i$  initiates shortening and a decrease in  $[Ca^{2+}]_i$  leads to relaxation of the sarcomeres. This mechanism of the myocardial contraction can be influenced by changing of outer conditions. This study will observe the effect of a bacterial sepsis on an isolated cardiomyocyte. It is well known (Kohl et al., 2005) that isolated cardiomyocytes can be used as model for cardiac excitation contraction coupling. Experiments on single cell level have the advantage to reduce the amount of influencing factors compared to *in vivo* conditions and thus allow to establish simple cause-effect relations. Therefore, single cell experiments on isolated cardiomyocytes were performed in this study.

### **1.3 Pathogenesis of the Reduction of Myocardial Contractility**

As mentioned in Chapter 1.2, sepsis is a major medical problem which is associated with high mortality rate. The main contributor to sepsis related morbidity and mortality is cardiac dysfunction, also called septic cardiomyopathy, causing systolic and diastolic dysfunction in both ventricles due to preload and afterload decrease (Muller-Werdan et al., 2006, Parrillo et al., 1990). On cellular level, the contractility of the cardiomyocytes is reduced so that the function of the heart as a pumping organ is compromised as a whole. A systematic vasodilatation leading to a refractory hypotension is characteristic in septic patients as well. It brings the myocardial oxygen supply demand ratio out of balance. This vicious circle continues until the rest of the body suffers from a systematic ischemia and multi organ dysfunction, which leads to death of the patient. About 20% of all septic patients with refractory hypotension die because of a low cardiac output under septic

cardiomyopathy (Fernandes et al., 2008). The treatment of septic patients without further compromising the already reduced function of the septic heart is, therefore, of high clinical relevance.

Although the pathophysiology of the septic cardiomyopathy is not fully understood, recent findings suggest that the innate immune defense plays an important role. The acquired immune defense system, led by B and T lymphocytes, is highly differentiated and can bind antigens specifically. The recognition of the pathogen and the production of adequate antibody through plasma cells, however, often take three to five days which is enough time for microorganisms to cause a fulminant sepsis. On the other hand, the innate immune defense system is less specific with only about some hundred different receptors. It can readily bind structures that are relatively uninfluenced by genetic variability, thus exhibiting patterns that are conserved and rarely change. These antigen structures are called pathogen-associated-molecular-patterns (PAMPs) (Medzhitov et al., 2000). PAMPs can be described as small molecular motifs conserved within a class of microbes. They are recognized by Toll-like receptors (TLRs) and other pattern recognition receptors (PRRs) in animals and plants. They activate an innate immune response, protecting the host from infection by foreign material. Common PAMPs include lipopolysaccharide (LPS, recognized by TLR4), bacterial flagellin (recognized by TLR5), lipoteichoic acid from Gram positive bacteria, peptidoglycan, and nucleic acid variants normally associated with viruses, such as double-stranded RNA (dsRNA, recognized by TLR3) and unmethylated CpG (Cytosin-Phosphate-Guanosin) motifs, abundant in microbial genomes (recognized by TLR9).

Bacterial lipopolysaccharide, an endotoxin found in the bacterial cell membrane, is considered to be the prototypical PAMP. It is the major component of the outer membrane of gram-negative bacteria, contributing to the structural integrity of the bacterium and protecting the membrane from the outer influence (Medzhitov, 2001; Pålsson-McDermott and O'Neill, 2004). 30% to 50% of all reported sepsis cases involve an infection with gram-negative bacteria which makes LPS clinically highly relevant as a PAMP (Rensing, 2003). Common gram-negative bacteria, which play important roles in modern medicine, are, for example, *Escherichia coli*, *Salmonella*, *Shigella*, *Pseudomonas*, *Helicobacter*, *Legionella*, *Neisseria*, *Hemophilus*, and *Klebsiella*. LPS, as described, acts as the prototypical endotoxin because it binds the CD14/TLR4/MD2

receptor complex, which promotes the secretion of proinflammatory cytokines in many cell types including cardiomyocytes, macrophages and B cells. (See Figure 1) LPS consists of a polysaccharide and a phospholipid section. (See Figure 2) The polysaccharide section, also called O antigen, has up to 50 repeating carbohydrate chains and can be used for serotyping of the bacterium. The rest can be categorized into the outer core, the inner core, and the phospholipid section (Lipid A). The Lipid A section (See Figure 2) is mainly responsible for the immune stimulating toxicity of LPS (Alexander and Rietschel, 2001; Lien et al., 2000; Medzhitov, 2001; Rensing, 2003; Schletter et al., 1995).

LPS is connected to the outer membrane of a bacterium through its Lipid A section and makes up about 75% of the outer layer of gram-negative bacteria (Alexander and Rietschel, 2001). If a bacterium breaks down due to the effect of antibiotics or lysis by the immune system, LPS is released. This is recognized by TLR4 (Medzhitov, 2001; Mukhopadhyay et al., 2004; Pålsson-McDermott and O'Neill, 2004). TLR4 consists of an extracellular leucine abundant region and an intracellular Toll/IL-1-Domain (TIR).

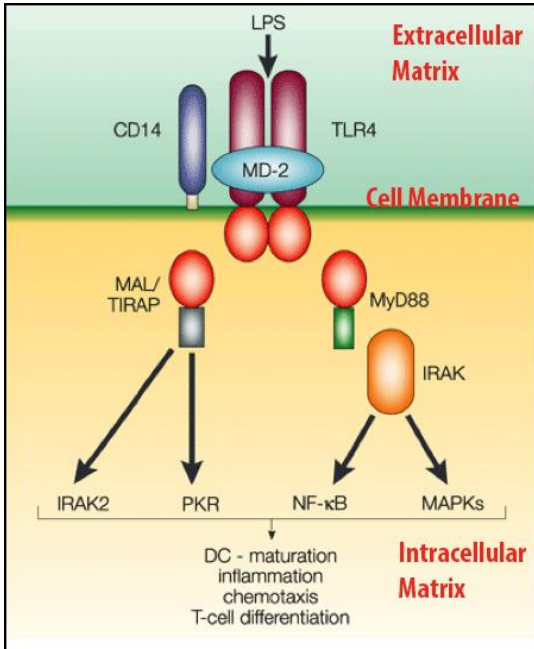


**Fig. 1:** Schematic Signal Cascade of LPS binding the CD14/TLR4/MD2 Complex (Buer and Balling, 2003)

The transmembraneous structure allows to transduct signals from the outside to the inside of a cell (Lakhani and Bogue, 2003; Medzhitov, 2001). The first structure that binds LPS is LPS-binding protein (LBP) which is secreted in the liver and circulates

freely in blood. Serum LBP binds the Lipid A section with high affinity and brings it to the CD14 molecule which is located on the cell surface (Schumann et al., 1990). After the combination of these three components (LPS, LBP, CD14), LPS can be loaded onto the receptor complex, which is composed of a TLR4 receptor and the extracellular adapter MD2 (Nagai et al., 2002, Schromm et al., 2001). MD2 is a glycoprotein that connects two TLR4 molecules on the extracellular side, and is an essential factor in the LPS signaling pathway.

Unlike CD14, MD2 binds TLR4 directly, although the presence of CD14 is needed to initiate the signal transduction of TLR4 in many cases, as Visintin et al. (2002) demonstrated. Namely, they showed a reduced responsiveness to LPS. On the contrary, mice with overexpression of CD14 showed more intensive inflammatory reactions (Ferrero et al., 1993). Still the fact that LPS induced some significant, though reduced, reactions in CD14 deficient mice suggested that there is a signaling pathway which does not involve CD14 and this could be demonstrated later (Godowski et al., 2005; Haziot et al. 1998; Jiang et al., 2005).

Through the binding of LPS to the TLR4 receptor complex, a signal pathway begins which then activates the transcription factor NF $\kappa$ B that increases the transcription of proinflammatory cytokines, such as TNF $\alpha$ , IL-1 $\beta$ , IL6, and IFN $\gamma$ .

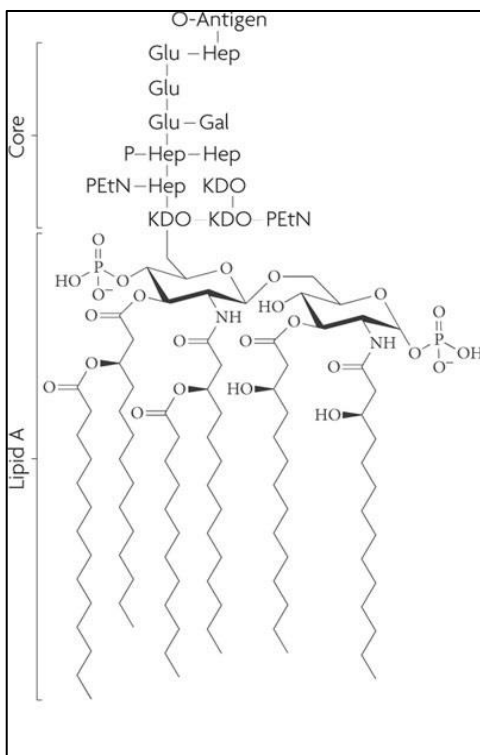


**Fig. 2:** The structure of *E. coli* LPS (Ruiz et al., 2009) LPS consists of a core section and a lipid A section. The Lipid A section is responsible for the toxicity of LPS.



In addition, the expression of the inducible NO-Synthase (iNOS) is increased. The expression and the secretion of these cytokines result in the reduction of contractility of the heart muscle, as clinically and experimentally demonstrated (Avlas et al., 2011; Baumgarten et al., 2006; Boyd et al., 2006; Kapadia et al., 1995; Muller-Werdan et al., 2006; Pagani et al., 1992). Baumgarten et al. furthermore demonstrated that isolated heart muscle cells treated with LPS showed reduced contractility with lower sarcomere shortening amplitude and prolonged duration of relaxation.

#### **1.4 Objective of this Study**

In this study the effect of bacterial sepsis caused by LPS should be observed on the cellular level. Murine cardiomyocytes should be isolated and incubated with or without LPS, thus simulating a septic shock. The hypothesis of this study was that LPS will reduce shortening of isolated cardiomyocytes and that this can be overcome by  $\beta$ -stimulation. This hypothesis should be tested quantitatively on single cell level. Therefore, isolated cardiomyocytes should be incubated in LPS and then stimulated by orciprenaline. Comparison of septic cardiomyocytes with and without  $\beta$ -stimulation should reveal the potency of  $\beta$ -stimulation on LPS treated cells.

## **2 Material and Methods**

### **2.1 Test Animals and Maintenance Conditions**

Male C57BL/6 mice were obtained from Charles River Deutschland GmbH (Sulzfeld, Germany). The mice were raised and maintained in full accordance to the current guidelines for use and care of laboratory animals. The animals were kept in cages made of polycarbonate, each measuring 365 x 207 x 140mm in size. The bottom was covered by Altromin Animal Hay Granulate (Altromin GmbH und Co. KG, Lage-Lippe, Germany). A constant living environment (temperature between 20°C and 22°C, relative air humidity at 50%, twelve hours shifting day and night circadian rhythm) was provided consistently for the mice. The cages were mounted in a mouse cage shelving system. Each cage could be pulled out of the shelf and attended separately. Separated ventilation for each cage was provided in order to guarantee optimal hygienic conditions. The animals were fed with clean tap water and a standard diet (Altromin for mice and rats). The amount was not limited. The young animals at the mentioned inbreeding facility were separated from their parent animals at the age of four weeks and were sorted and separated by gender.

### **2.2 Description of the Experimental Method and Cell Groups**

Ventricular cardiomyocytes were isolated freshly from murine hearts for each *in vitro* experiment. The main objective was the precise measurement of the extent of sarcomere shortening under control conditions and under the influences of various stimulating factors which are to be introduced later in detail.

Isolated cardiomyocytes were divided into three groups. The control measuring of sarcomere was done with the newly isolated cells that were suspended in a Tyrode's solution (See Table 2.1). The remainder of the cells was incubated in culture mediums, separated in two groups, for 6 hours after which the experiment was performed. The cells of the first group were initially stimulated with LPS and were incubated in order to simulate a septic condition. The second group was incubated without an addition of a stimulant.

### 2.2.1 Isolation of Ventricular Cardiomyocytes

The isolation of ventricular cardiomyocytes was carried out enzymatically applying a modified Langendorff apparatus, with which the heart tissue was anterogradely (through the coronary arteries) perfused, with solutions containing digestive enzymes. Each of the following steps was standardized and carried out under identical conditions in order to guarantee consistency of the outcome.

The mice were anaesthetized in an exsiccator. After sedation, the animals were sacrificed by cervical dislocation and were fixed for dissection. From each dissected mouse, the heart was extracted in a cautious yet timely manner so that the tissue would stay as fresh as possible. The heart was then transferred to a Petri dish which was filled with EGTA-Tyrode's solution. EGTA (Ethylene Glycol Tetraacetic Acid) had the function of binding the extracellular calcium ions and decreasing both the extracellular and intracellular calcium ionic concentration so that the autonomic myocardial contraction would cease during the course of the cell isolation and afterwards during the experiment. The composition of the solutions is described in Table 2.1 and 2.2. The solutions were prepared following the work of Tiemann et al. (2003)

The aorta was then exposed under a stereo microscope. The surrounding tissue material, consisting mainly of connective tissue and lung parenchyma, was removed with small scissors, carefully so that the myocardium, coronary arteries, and the aorta could be kept undamaged. The aorta was cleanly cut at the distal end of the aortic arch. The opening of the aorta was then spread sideways with two small tweezers. The aorta was mantled on a glass cannula which was fixed on the Petri dish and had an outer diameter of 1.1 mm and an inner diameter of 0.8 mm.

The aorta was pulled up so that the end of the glass cannula would be pushed into the lumen of the left ventricle, breaking the aortic semilunar valves. A silk thread was then wound around the aorta and the glass cannula proximal to the brachiocephalic artery and was tied so that the aorta was fixed on the glass cannula airtight (See Figure 3). The glass cannula with the heart was then taken off from its fixation and was docked onto the Langendorff perfusion system. It was made sure that the system, including the glass cannula, was air bubble free to prevent a possible air embolization of the coronary arteries.



**Fig. 3:** Mouse heart with aorta mantled on the glass cannula. The coronary arteries appear to be free of blood.

1. coronary arteries
2. Langendorff cannula

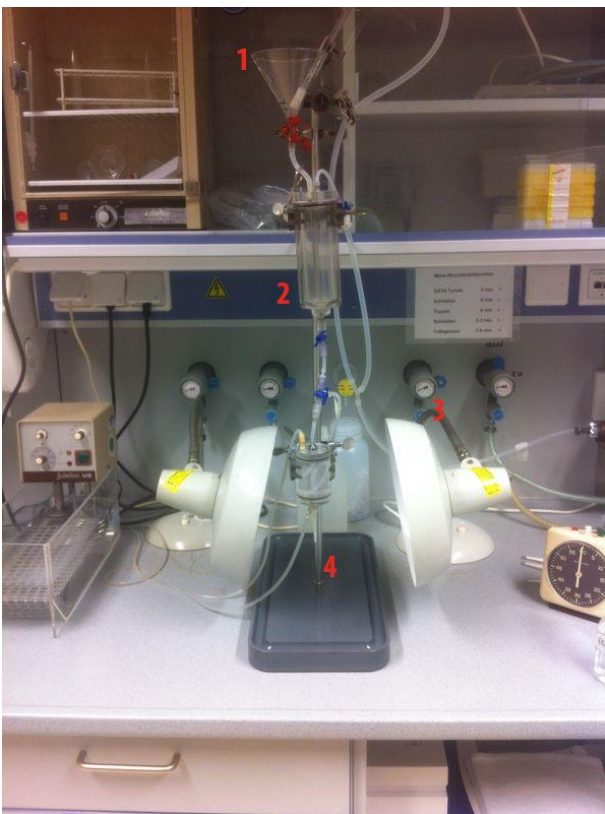


**Fig. 4:** Langendorff perfusion system for cell isolation

1. glass funnel
2. high pressure chamber
3. pressure regulator
4. Langendorff cannula

The Langendorff perfusion system had three main functions: oxygenation and warming up the perfusion solution up to 36 °C as well as creating the necessary perfusion pressure of 100 to 200 mm H<sub>2</sub>O (See Figure 4).

It consisted of a funnel with a glass frit which oxygenated the perfusion solution. When the connecting hose between the funnel and the high-pressure chamber was opened, the oxygenated solution flew into the chamber. During this flow, the pressure in the chamber was set equal to the air pressure outside the system, so that the solution would fill the chamber following gravitation. When the chamber was full, the connecting tube to the funnel was shut tight, and pressure was applied to the chamber. The heating device for the solution was a flexible rubber hose inside a second chamber that was supplied with circulating warm water from an external bath with a controlled heating system. The heating water from the bath and the perfusion solution were completely separated from each other. While flowing through the heating chamber the solution was warmed up to 36°C. From there, a silicon hose led to the glass cannula connected to the heart so that the solution could be perfused into the coronary artery system while the pressure of the chamber was being applied.

Two external lamps were used in order to keep the glass cannula and the heart surface warm as well because the room temperature was constantly at a lower level than 36°C, which would result in radiation of heat from the myocardial surface, causing it to become cooled down. The lamp's position was also varied so that the ideal temperature level was reached. The temperature of the heart's surface was controlled every 3 to 4 minutes so that 35-36°C could be kept consistently.

Before the beginning of a Langendorff perfusion, a higher pressure was shortly applied to the system (ca. 5 s) so that the remaining blood in the heart lumens and the coronary arteries could be forced out in an attempt to guarantee a constant perfusion. After this, characteristically transparent coronary arteries filled with the clear solution could be observed by naked eye (See Figure 3). The pressure of the perfusion system was adjusted to the standard level (100 to 200 mm H<sub>2</sub>O) shortly after this initial maneuver and set to an appropriate perfusion speed.

The perfusion speed and the temperature of the heart surface were constantly controlled in order to avoid overheating of the heart, which would result in: 1. an overly increased enzymatic activity, causing the cells to be "digested" rather than isolated, 2. heat induced reduction of the overall cell vitality. By adjusting the pressure level, an appropriate perfusion speed was chosen. Experience shows that keeping a constant temperature of between 34 and 36°C (with the optimum of 35°C, measured on the

surface of the heart with an electronic thermometer) resulted in the best isolated cells, qualitatively and quantitatively.

In the initial phase of the perfusion, the heart was perfused with EGTA-Tyrode's solution for 5 minutes (See Table 2 for exact composition). This would result in building calcium chelate complexes, reducing the extra cellular calcium level significantly.

After this, a second solution was introduced to the system. To change the perfusion solution, the pressure system was halted and the remaining solution was let out of the chamber. After this, the already oxygenized new solution in the funnel could flow into the chamber. The solution was bubbled with 100% O<sub>2</sub> for at least 30 seconds in order to guarantee a sufficient supply of O<sub>2</sub> to the cardiomyocytes. The second solution contained a potassium concentration equal to the cytoplasm (See Table 3 for exact composition). This increase of extra cellular potassium level resulted in a membrane potential of 0 mV and prevented potassium efflux from the cells. Fast sodium channels and voltage operated calcium channels became inactivated. The autonomous contraction of the cells ceased, reducing the energy consumption of the cells, leading to higher chance of survival. This second solution was applied for 5 minutes.

**Tab. 2:** composition of EGTA-Tyrode solution and measurement Tyrode for the isolation, perfusion and measurement of cardiomyocytes

<b>Substance</b>	<b>EGTA-Tyrode's</b>	<b>Measurement Tyrode's</b>
KCl (Merck)	4 mM	4 mM
NaCl (Merck)	135 mM	135 mM
CaCl <sub>2</sub> (Merck)	-	1.8 mM
MgCl <sub>2</sub> (Merck)	1 mM	1 mM
HEPES (Merck)	1 mM	1 mM
BSA (Sigma)	-	1 mg/ml
Trypsin Inhibitor (Sigma)	-	0.017 mg/ml
Glucose (Merck)	-	9 mM
EGTA (Serva)	2.6 mM	-
pH (NaOH)	7.4	7.4

**Tab. 3:** composition of perfusion solutions with or without the addition of enzymes trypsin or collagenase

Substance	Potassium	Trypsin Solution	Collagenase
KCl (Merck)	10 mM	10 mM	10 mM
NaCl (Merck)	4 mM	4 mM	4 mM
CaCl <sub>2</sub> (Merck)	0.02 mM	0.02 mM	0.02 mM
MgCl <sub>2</sub> (Merck)	1 mM	1 mM	1 mM
HEPES (Merck)	4 mM	4 mM	4 mM
Glucose (Merck)	9 mM	9 mM	9 mM
Potassium-glutamate	130 mM	130 mM	130 mM
Trypsin (Roche)	-	0.4 mg/ml	-
Collagenase Type L	-	-	0.375 mg/ml
Polymyxin B (Sigma)	-	-	100 U/ml
pH (KOH)	7.4	7.4	7.4

Then, the actual enzymatic dissolving process of the cell-cell connections started. First, the heart was perfused with a trypsin solution for 10 minutes. While identical to the already mentioned potassium solution in its composition, it had an additional ingredient of 0.4 mg/ml trypsin (Roche, Mannheim), which is a digestive enzyme extracted from the cow's pancreas. Trypsin dissolves specific peptide connections on the carboxyl group of Arginine or Lysine. With the introduction of trypsin solution to the system, the perfusion speed was significantly reduced, and the solution leaking from the heart increased in its viscosity dramatically which could be observed macroscopically.

Thereafter, the potassium solution was again perfused shortly for 2 to 3 minutes in order to wash out the enzyme to prevent its prolonged activity. Now the collagenase enzyme solution was perfused into the heart for 10 to 12 minutes. This was, again, the potassium solution, this time, with the addition of collagenase Type L (Sigma-Aldrich, Steinheim, See Table 3). This enzyme was isolated from the gram-negative bacteria *Clostridium histolyticum*. This particular type of collagenase clears the specific peptide sequence of GLY-PRO-X-GLY-PRO, which occurs frequently in protein abundant collagen. X in the sequence can be any amino acid. Since the enzyme was isolated from gram-negative bacteria, it was feared that the solution might contain LPS contaminations. In order to eliminate this possible artifact, the solution was mixed with the Polymyxin B solution (Sigma-Aldrich, Steinheim) in a concentration of 100 U/ml. Polymyxin B is a peptide-

antibiotic substance which consists of 11 amino acids. It has a high affinity to LPS and can bind free LPS particles, causing it to lose its toxicity (Warner et al., 1985).

During the perfusion with the collagenase solution, the perfusion speed increased rapidly toward the end, which was taken as a sign of loosened cell-cell connections. After the Langendorff perfusion, an incision was made through the lower part of the heart in order to let out the remaining solution in the cardiac ventricles. The heart was detached from the glass cannula and transferred to a small glass beaker filled with measurement Tyrode's solution at 36°C. The heart was then chopped up mechanically with a pair of small scissors. This suspension of shredded tissue and cells was run through a gauze filter into three glass centrifuge tubes in approximately equal volumes. The tubes were then centrifuged shortly so that each tube, in an ideal situation, displayed brown-pink colored pellet on the bottom. Now, each of the three pellets was mixed with the Tyrode's solution. This new suspension was allowed to sediment for 10 minutes. The color of the pellet turned to yellow. The pellet was resuspended and the solution with the cells was filled into a 36°C preheated Erlenmeyer flask with a Pasteur-Pipette for the control measurement. The flask was provided with oxygen and was shut air-tight.

### **2.2.2 Incubation of the Isolated Cells**

The remaining two groups of cells in two separate centrifuge tubes were prepared for incubation. Each group was mixed with 2 ml of culture medium (See Table 4). One group was administered with LPS (See 2.2.2.2), in order to simulate an infection caused by gram-negative bacteria. Both groups were stirred and were separately moved to Petri dishes with 5 cm diameter. These were then kept in an incubator at 37°C and an air CO<sub>2</sub> level of 5%. Our study group could already show in the past that the shortening length of murine cardiomyocytes under identical experimental conditions was not reduced even after 6 hours of incubation in the culture medium. (Baumgarten et al., 2006; Knuefermann et al., 2008).



### 2.2.2.1 The Culture Medium

The culture medium is a short term culture medium, where the cells could survive up to 12 hours under the given circumstances. The composition of the solution is to be seen on the Table 4.

**Tab. 4:** composition of the short term culture medium for the ventricular cardiomyocytes

Substance	Provider	Percentage
Fetal Bovine Serum	Gibco, Grand Island, NY,	5%
Minimal Essential Medium	Gibco, Grand Island, NY,	5%
Gentamicin	Gibco, Grand Island, NY,	50 µg/ml
Dulbecco's Mean Eagle	Gibco, Grand Island, NY,	ad 100%

### 2.2.2.2 Lipopolysaccharide

As mentioned in 2.2.2, a group of isolated cardiomyocytes was cultured with an addition of LPS (Sigma-Aldrich, St. Louis, MO, USA, L-3024) from the bacterium *Escherichia coli*-Serotype O111:B4. It consists of a Lipid A-component and a Polysaccharide chain (See Figure 2). The lyophilized and dry LPS powder was resuspended in Tyrode's solution to a final concentration of 1 mg/ml and was stored at 4°C. Then, one Petri dish containing the isolated cells and 2 ml of culture medium was pipetted with 20 µl of the LPS solution so that the culture medium would have the LPS concentration of 10 µg/ml (See 4.1).

## 2.2.3 Measurement of Sarcomere Shortening

### 2.2.3.1 Experimental Setup

The setup is displayed in Figure 5.

The equipments that are needed for the measurement of sarcomere shortening are divided into three groups according to their functions.

1. Creating the optimal conditions for the cells during the measurement:

The cells were brought into the center of a round and flat test chamber. A water circulatory system which was connected to the chamber guaranteed a constant temperature of 36 °C in the test environment. The supply of sufficient nutrition for the cells was obtained by a continuous perfusion with Tyrode's solution.

2. Generation of external electrical stimulation:

A computer with the software Clampex® (Axon Instruments, Union City, CA, USA) was equipped with a Digital-Analog converter. It was connected to an electric pulse stimulator (SD 9, Grass Technologies, West Warwick, RI, USA) that could produce electrical stimuli with a predefined voltage and length. The stimulator was connected directly to the stimulation electrodes that reached into the perfusion solution in the measuring chamber with the cells.

3. Registration and processing of the sarcomere shortening:

The test chamber was placed on the stage of an inverted microscope. The cells were visualized by a special video camera (MyoCam, IonOptix, Milton, MA, USA). The video images were digitized and then transferred to a computer equipped with the IonWizard software (IonOptix). This software allowed to save the images in a file. The further processing is explained in Chapter 2.4. In order to eliminate possible vibration of the set up caused by an external force, for example by hand, the microscope was mounted on a shock absorbing table. This table consisted of a metal frame on which a stainless steel basin was placed on shock absorbing rubber dampers. The basin was filled with quartz sand which carried a 3 cm thick granite plate. This granite plate formed the desktop.



**Fig. 5:** Experimental Setup

1 Microscope Axiovert 100 TV, 2 Ion Optix MyoCam, 3 Perfusion system, 4 Julabo F10 warm bath, 5 HyoFlo suction pump, 6 Ion Optix HyperSwitch, 7 Transformer for the xenonlamp (not used during this experiment), 8 Ion Optix Fluorescence system interface (not used during this experiment), 9 Ion Optix camera control unit, 10 Amplifier, 11 Control monitor for data acquisition, 12 Grass SD 9 stimulator, 13 Transformer for the lamp, 14 Control monitor for controlling of the electrical stimulation.

### 2.2.3.2 Test Chamber

The test chamber was manufactured out of acryl by the mechanic workshop of the Physiological Institute II (See Figure 6). It was circular and had an outer diameter of 50 mm. It was fixated on the object stage of the microscope by screws. In the center of the measuring chamber was a hole of 10 mm diameter. On one side this hole was closed by a microscope cover slip, forming the bottom of the small chamber. The cover slip was attached to the experimental chamber using a two-component glue. The microscopic cover slip allowed a visualization of the cells with microscopic objectives of high

resolution. To keep the temperature of the solution with the cells at 36 °C a small channel was milled around the central chamber for the cells. This channel was permanently perfused with warm water pumped by a heated water bath. The temperature of the water was controlled via a feedback loop with its sensor in the solution of the cells. A continuous perfusion with the above mentioned prewarmed Tyrode's solution was provided for the cells during the course of the experiment. The inflow of the perfusate was driven by gravity, whereas the outflow was provided by application of negative pressure to a glass capillary. The inflow and the outflow speed were kept in a balance so that the fluid level in the chamber would stay as constant as possible. Through these mechanisms a consistent experimental environment could be provided so that the cells could be measured for about 30 minutes without deteriorating.

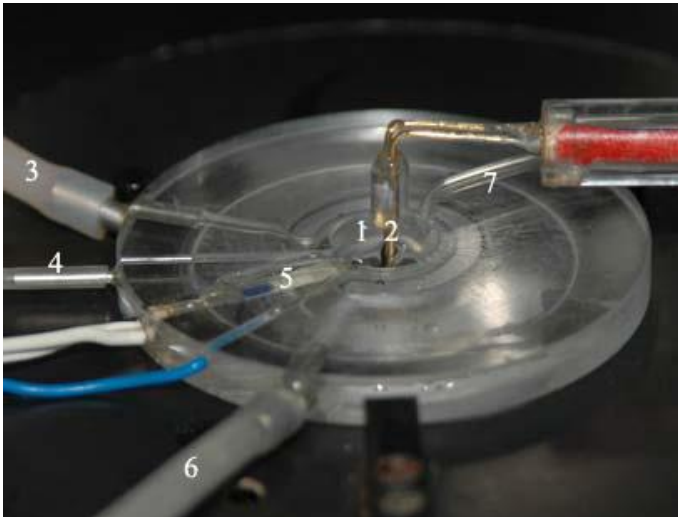


**Fig. 6:** Test Chamber

1. measuring area
2. stimulation electrodes
3. warm water outlet
4. perfusion inlet
5. temperature sensor
6. warm water inlet
7. glass suction capillary

### 2.2.3.3 Coating of the Measuring Area with the Cardiomyocytes

A continuing perfusion with measurement Tyrode's solution and a continuing suction would cause the cells to drift away from their positions, making it impossible to measure their sarcomere shortening. In order to overcome this problem, the cells were adhered to the bottom of the measuring area by the protein laminin (Sigma-Aldrich), a major protein of the basal lamina. Laminin was dissolved in the measurement Tyrode's at a concentration of 8 µg/ml. Three drops of this solution were pipetted on the glass bottom of the measuring area. After 6 minutes, the fluid in the measuring area was sucked away.

Afterwards, the cell suspension was pipetted onto the measuring area. Another 6 minutes were given so that the cells could attach themselves to the bottom with the help of laminin. The warm water circulation was turned off throughout this phase, because it would have resulted in overheating of the chamber otherwise, which would lead to deterioration of the cells.

#### **2.2.3.4 The Perfusion System**

In order to obtain a reliable, reproducible measurement results, it was essential to optimize the perfusion. The perfusion should not be too fast, lest the cells drift away, nor should it be too slow that the cells would not receive sufficient oxygen and nutrition. Moreover, the perfusion should be continuous and not periodical, therefore the suction also had to be continuous. Experience showed that an unbalanced perfusion normally results in irregular flow around the cells, causing the cells to detach from the bottom and to drift away. To build up a balanced flow, a reservoir of the perfusion solution was provided in a form of a holder for a 50 ml perfusion syringe which was mounted 30 cm above the measuring chamber, to establish a gravity gradient. The speed of the perfusion was regulated using an infusion drop regulator (Exadrop®, Braun, Melsungen) which was inserted between the syringe and the chamber. The speed was kept at 70 drops per minute. Before entering the experimental chamber the perfusion buffer was warmed to 36 °C using a heat exchanger. The heat exchanger was coupled to the same water bath that supplied the measurement chamber. The negative pressure necessary for the suction of the perfusion solution was generated by a suction pump (HyoFlo, Herts, UK) which was connected to an empty jar with the capacity of about 10 liters. This jar was connected to the glass capillary by a silicon hose.

#### **2.2.3.5 The External, Electrical Stimulation**

In order to induce a controlled shortening of the cardiomyocytes, they were stimulated by electrical pulses to elicit action potentials. As mentioned above, this electrical stimulation was applied through two 0.8 mm thick gold wires that were parallel to each other and were fastened with an acryl molding. This was attached to a micro manipulator

so that the electrodes could be moved around in the measuring area. Under the microscopic control, the electrodes were positioned so that the cell to be measured was located between the electrodes. The electrodes were connected to an external stimulator set. Each stimulus consisted of a voltage of 30 V and duration of 0.4 ms. The cells were stimulated with changing frequencies. There was a pause of 30 seconds between the stimulus trains. The respective order of the frequencies was 0.5, 10, 1, 8, 2, 6 and 4 Hz. The trigger signal which drove the stimulator was given by the Clampex Software which was installed on a computer equipped with an Analog-to-Digital converter. Each stimulus train consisted of 20 pulses.

### **2.2.3.6 $\beta$ -Stimulation with Orciprenaline**

Orciprenaline, also known as metaproterenol, is a moderately selective  $\beta$ -adrenergic receptor agonist which mainly stimulates the  $\beta_1$ -adrenoceptors but also  $\beta_2$ -adrenoceptors to some degree. However,  $\beta_2$ -adrenoreceptors are not expressed in the myocardium. By binding  $\beta_1$  adrenoceptors it contributes to stimulation of intracellular adenylylcyclase, the enzyme which catalyzes the conversion of ATP to cAMP. Increased cAMP levels are associated with the phosphorylation of sarcolemmal calcium channels and activating the calcium pump in the cardiomyocytes (Honerjäger, 1989). This causes an increase of intracellular calcium level, which results in the positive chronotropy, bathmotropy, dromotropy and inotropy. Orciprenaline found its use in the emergency medicine for intravenous application in patients with acute circulation failure. However, as more specific  $\beta_1$ -adrenoreceptors (i.e. dobutamine) became available, its use has been limited to the treatment of acute asthma attacks. Orciprenaline was used in this study in the form of orciprenaline sulfate (Boehringer Ingelheim Pharma GmbH, Ingelheim am Rhein), mixed with the Tyrode's solution in the concentration of 0.3  $\mu\text{g/ml}$  which is the serum concentration of a normal patient of 75 kg after the intravenous application of one ampule of Alupent® in the emergency medicine. The Tyrode's solution with orciprenaline was perfused through the experiment chamber during the stimulation of the cardiomyocyte. Orciprenaline was chosen in this study instead of other, more specific  $\beta_1$ -agonists because of the stability against oxidation (instruction leaflet, Boehringer

Ingelheim) when used as solution and the easy access to the substance for experimental purposes.

#### 2.2.4 The Principle of the optical Sarcomere Length Measurement

Both skeletal and cardiac muscles belong to the cross-striated muscles, due to the characteristic pattern of the actin and myosin filaments in the sarcomere. Therefore, the cardiomyocytes exhibit a striated pattern of alternating dark and light bands in a light microscope. The distance between one dark band and the next resembles the length of a sarcomere. Through the video camera that was attached to the inverted light microscope (Zeiss Axiovert 100 TV, Carl Zeiss, Oberkochen, Germany) the dark and bright bands in a defined area of interest of a cardiomyocyte could be displayed, registered and processed. The local distribution of the striation pattern was evaluated for its brightness and thus transformed to a sinusoidal curve (See 3 in Figure 7). The wavelength of this sinusoidal curve was consistent with the respective sarcomere length (See Figure 7).

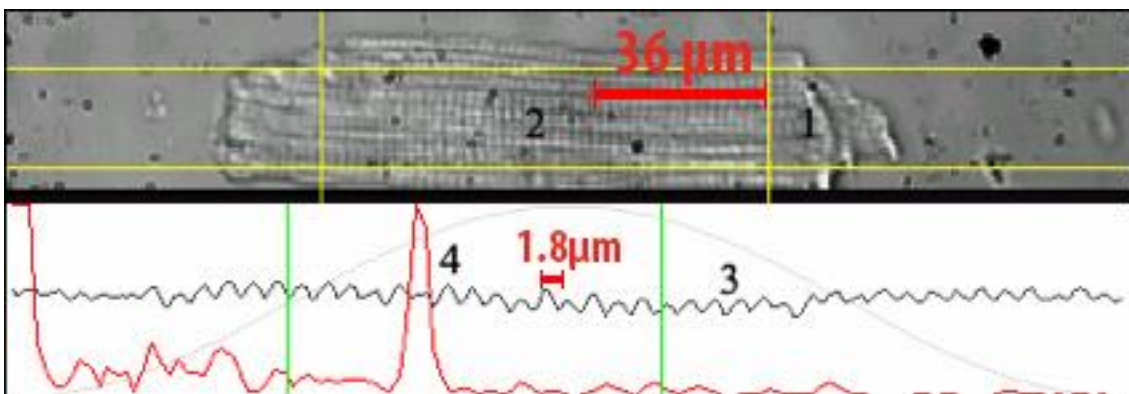


**Fig. 7:** Video image of a cardiomyocyte with its power spectrum. Software IonWizard (IonOptix, Milton, MA, USA) 1. Cardiomyocyte, the scale (36  $\mu\text{m}$ ) indicates 20 sarcomeres, 2. Region of interest, 3. Oscillation Curve, the scale (1.8  $\mu\text{m}$ ) indicates a single sarcomere length, 4. Power Spectrum (red line).

The information from this wave was extracted by calculating a Fast-Fourier Transformation (See red line, Figure 7). The resulting power spectrum formed a peak at the absolute sarcomere length (See 4, Figure 7). A sarcomere shortening caused the peak of the power spectrum to drift. The camera captured the images at a frequency of 240

Hz in order to follow the fast alterations of the sarcomere length during the murine action potential.

Before the recording started, optimal cells were selected. An important criterion for the usability of the cells was the physiological, rectangular shape of the cell. By exact alignment of the sliding stage of the microscope and the camera angle, a cell was positioned so that the entire cell was displayed in the field of vision and the striation pattern was in line with the horizontal axis of the image. The cell was stimulated a couple of times by hand, using the manual function of the stimulator to make sure that the cell contracted properly without losing its adherence to the bottom of the chamber. Then, using the software, a region of interest was chosen. This rectangular area contained the part of the cell that had well shaped sarcomere structure with good contrast. After this, the measurement and data acquisition could be initiated by starting the electrical stimulation program and the data acquisition program.

## **2.3 Data Acquisition and Analysis**

The sarcomere shortening in the above mentioned frequency sequences was registered, recorded and analyzed with the help of the software IonWizard (IonOptix, Milton, MA, USA).

### **2.3.1 Analysis of the Data Set Acquired during the Sarcomere Shortening**

The measured and calculated sarcomere lengths were saved as events on a timeline, in real time length of the experiment. This caused every stimulation frequency to have a characteristic appearance. The last five shortenings of a pulse train were marked manually and were averaged. Only the last five shortenings were taken into account, because our group (Tiemann et al., 2003, Baumgarten et al., 2006; Schumacher, 2006; Vervölgyi, 2007) has shown in previous studies that the early stimulations in a given pulse train is a part of the staircase and not in steady state. In addition, only the shortenings fulfilling the following criteria were taken (See Figures 8, 9, 10): All 20 shortenings in a train had to be faultless, without spontaneous shortening in-between. In



addition, only the pulse trains were considered that did not have any shortening immediately before and after.

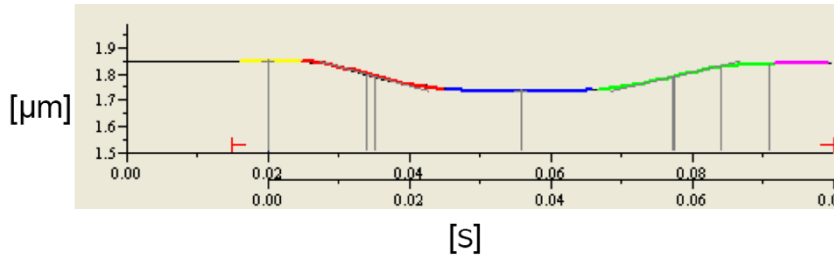


**Fig. 8:** A plot of the average sarcomere shortening, calculated from the last five shortenings in a pulse train. The x axis represents time in seconds, the y axis the sarcomere length in  $\mu\text{m}$ .

From this representative shortening, the program calculated five different parameters that were needed for the statistical analysis of the experiment: the resting sarcomere length, the shortening amplitude, the shortening and relaxation speed, and the shortening duration.

### 1. Resting Sarcomere Length

The sarcomere length at a relaxed state could be measured by the program automatically. At lower stimulation frequencies, the cardiomyocytes had sufficient time to relax completely (usually  $< 6$  Hz). At higher frequencies, however, the cells did not have enough time to return to their resting state, so that the program calculated a shorter resting sarcomere length here. This had to be corrected manually.

### 2. Shortening Amplitude

The shortening amplitude was calculated by IonWizard. The program took the difference between the resting sarcomere length and the minimum of a shortening curve. Because of the already mentioned phenomenon of the cells not returning fully to their resting length at higher frequencies, the shortening amplitude at these frequencies were not correctly calculated by the program. (See Figures 9, 10 and 11) Therefore, the difference between the manually measured resting sarcomere length

and the one measured by the program at these frequencies was added to the amplitude.

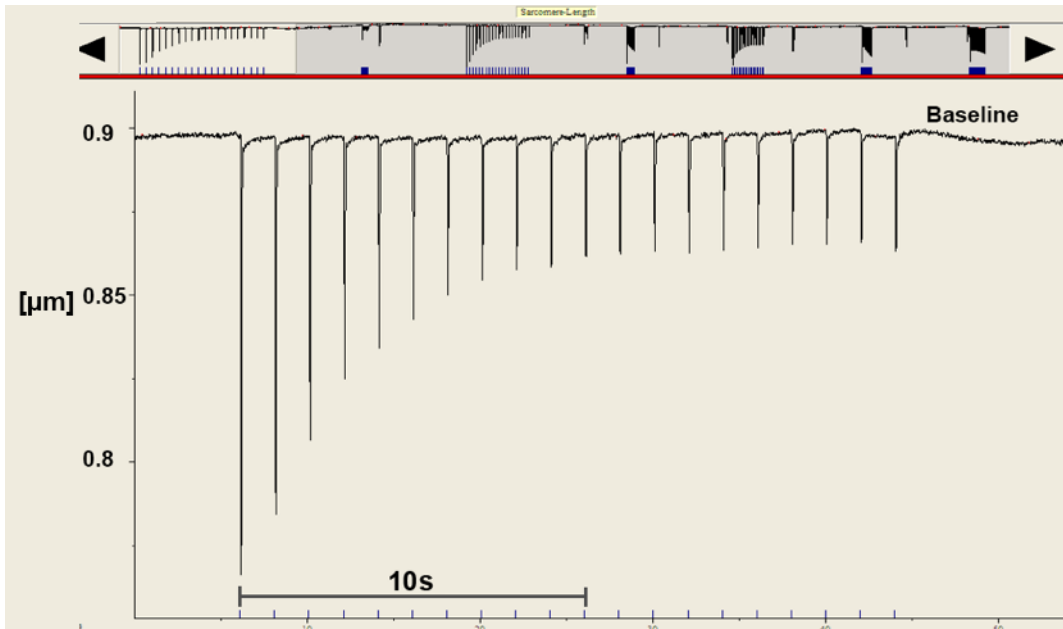


**Fig. 9:** 1 Hz, Baseline returning fully to the resting state position. The x axis represents time in seconds, the y axis the sarcomere length in  $\mu\text{m}$ .

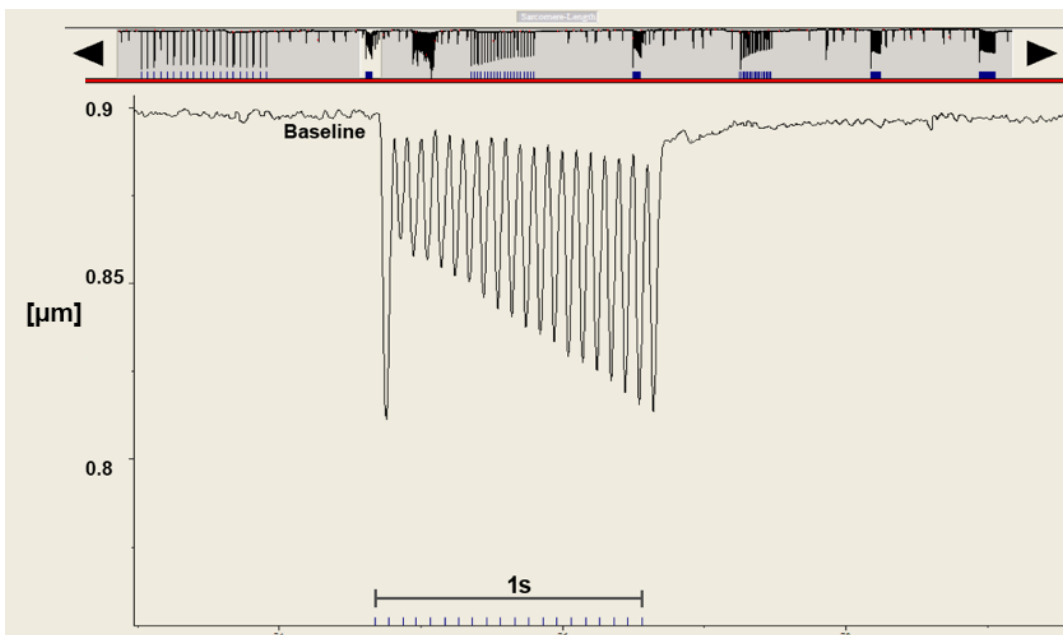


**Fig. 10:** 10 Hz, Baseline not returning fully to the resting state position. The x axis represents time in seconds, the y axis the sarcomere length in  $\mu\text{m}$ .

### 3. Shortening Speed

The maximal shortening speed was calculated by the program. It was the maximum of the first derivative of the descending part of a shortening curve.

#### 4. Relaxation Speed

Similar to the shortening speed, this was calculated as the maximum of the first derivative of the ascending part of a curve by the program.

#### 5. Shortening Duration

This was calculated by the program. It was the duration from the beginning of the contraction to the point where the sarcomere length had recovered to 90% of its original length.

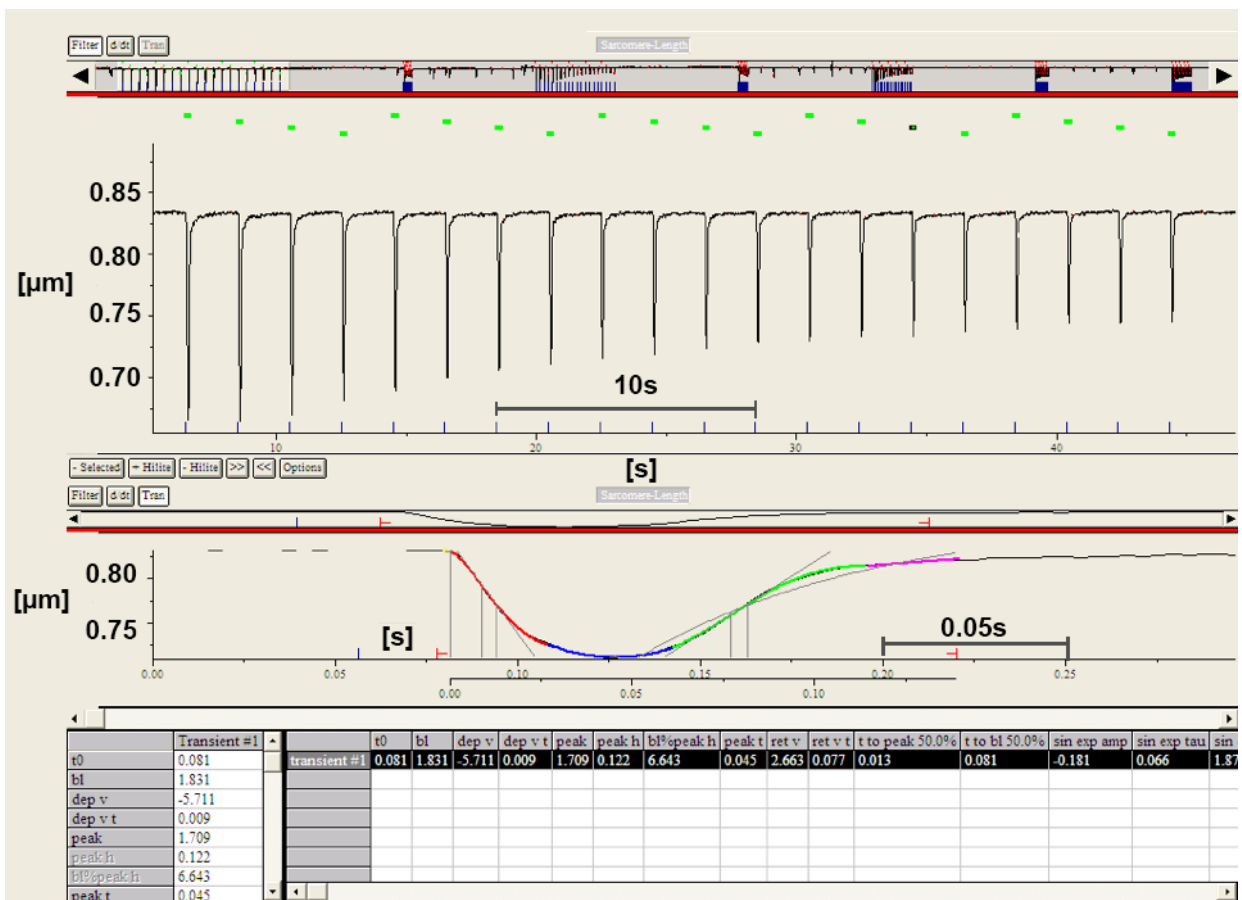


**Fig. 11:** IonWizard interface screen shot. On top of the screen a pulse train with 20 shortenings at 1 Hz can be seen. From these, the last 5 were selected and plotted as a single graph. The graph and the average parameters are seen on the bottom of the screen. The numeric table can be exported as a data set. The x axis represents time in seconds, the y axis the sarcomere length in  $\mu\text{m}$ .

### 2.3.2 Statistics

The numeric data sets produced by IonWizard were exported as text data (\*.txt). They were then summarized into a Microsoft Excel Table using Igor® (WaveMetrics Inc., Lake Oswego, OR, USA) and were sorted into 6 groups. In addition, the mean and the standard deviation were calculated. Then, the data sets were statistically organized and were plotted using the software Prism 3.0 (GraphPad Software, San Diego, USA). In order to test the differences between groups, a multi factor variance analysis (two-way ANOVA) with the following Holm-Sidak multiple comparison test was performed with all 6 groups at the same time. The arithmetic averages of the data sets were displayed as function of the standard error of the mean (SEM). The significance was defined as:

$p > 0.05$  not significant

$p < 0.05$  significant

## 3 Results

### 3.1 The Number of Test Animals used

A total of 49 test animals were used in this study. Only 33 successful preparations, delivering stable isolated cardiomyocytes were taken into the statistics. The reasons for the discrepancy are the following: First, some hearts and their coronary arteries were injured during the preparation so that the Langendorff perfusion was not possible to start with, since the “hole” somewhere on the myocardium or coronary artery let too much perfusion solution out. This made building up the necessary perfusion pressure impossible. Second, sometimes the excision of the aorta was too proximal to the heart so that mantling the heart on the glass cannula and fixing it with a thread was difficult. Third, the strict observation of the temperature and the perfusion speed during the Langendorff perfusion was not always successful. If, for instance, the temperature was above 39°C, the enzymes seemed to demonstrate greater activity than expected, so that the cardiomyocytes were literally “digested” which resulted in necrotic cells inadequate for *in vitro* experiments. On the other hand, if the temperature was below 35°C, the cell-cell contacts were not fully dissolved so that the isolation itself was unsuccessful. With more experience and perfection of manual skills, these failures could be eliminated and reliable quality of isolated cells could be achieved regularly.

### 3.2 Cell Groups

As mentioned in 2.2, cardiomyocytes isolated from C57BL/6 mice in the age of between 12 and 20 weeks were sorted into a total of three groups. The freshly isolated cells suspended in Tyrode's solution made the first group. The remainder of the cells was incubated in culture mediums, separated in two groups, for 6 hours after which the experiment was performed. The cells of the first group were incubated with LPS. The second group was incubated without an addition of a stimulant but otherwise in same conditions. All three groups were tested under microscope with or without the influence of the  $\beta$ -receptor agonist Orciprenaline. Therefore, a total of 6 groups were tested and the statistical results are listed below.

### 3.3 Original Registrations

To give an impression of the shortening behavior of the cardiomyocytes, averaged original recordings obtained in Tyrode's solution (See Figure 12A) and after incubation in culture medium with LPS (See Figure 12B) are displayed. These representative stimulation frequencies were chosen to demonstrate the frequency dependent post-rest behavior (0.5, 6, 10 Hz, See Figures 12, 13, 14 and 15). In a pulse train, the first shortening after a resting state of 30 seconds (called the "post rest" shortening) always had the greatest amplitude. After this, the amplitudes of 0.5 Hz to 4 Hz showed a "negative staircase" pattern, which means that the amplitudes within a pulse train decreased until reaching the steady state (See Figure 12). Then, from 6 Hz onto higher frequencies, a "positive staircase" pattern could be observed (See Figure 14). This phenomenon is consistent to what our study group described earlier (Tiemann et al., 2003).

This switching from negative to positive staircase was not observed in cardiomyocytes stimulated with LPS. In culture medium, they showed a negative staircase pattern at all 7 frequencies. Furthermore, the amplitude of shortening was clearly smaller after the incubation in culture medium with LPS (See Figure 14).

To visualize the time course of the staircase the following function (3.1) was fitted to the minimum of the averaged shortenings. The time constants  $\tau_1$  and  $\tau_2$  characterize the steepness of the negative ( $\tau_1$ ) and positive ( $\tau_2$ ) staircase.

$$y = (ss_1 - (ss_1 - \text{postrest})^{x/\tau_1}) + (ss_1 - ss_2)^{x/\tau_2} - (ss_1 - ss_2)$$

**Formula 3.1:** Formula for the calculation of the time constant  
 postrest: the minimum sarcomere length of the first Shortening after a resting state  
 ss1: sarcomere length of the second shortening at the minimum  
 ss2: sarcomere length at equilibrium (at 20th shortening at the minimum)

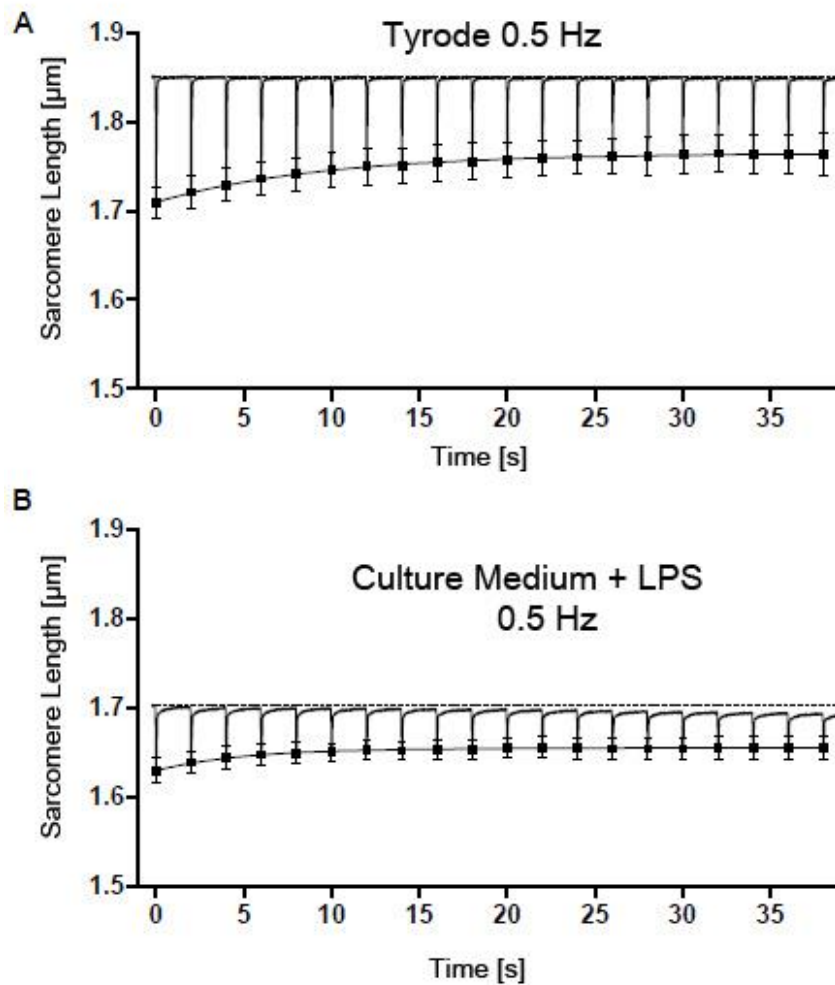


**Fig. 12:** Averaged original registrations of sarcomere shortenings of isolated cardiomyocytes of C57BL/6 mice during 20 external stimulations at 0.5 Hz. (A) shows the average of freshly isolated cells suspended in Tyrode's solution (n=45). (B) shows the average of shortenings of cardiomyocytes incubated in culture medium with LPS for 6 hours (n=18). Standard error is marked. The nonlinear regression curve was calculated with the formula 3.1. For both groups the "negative staircase" pattern can be seen.

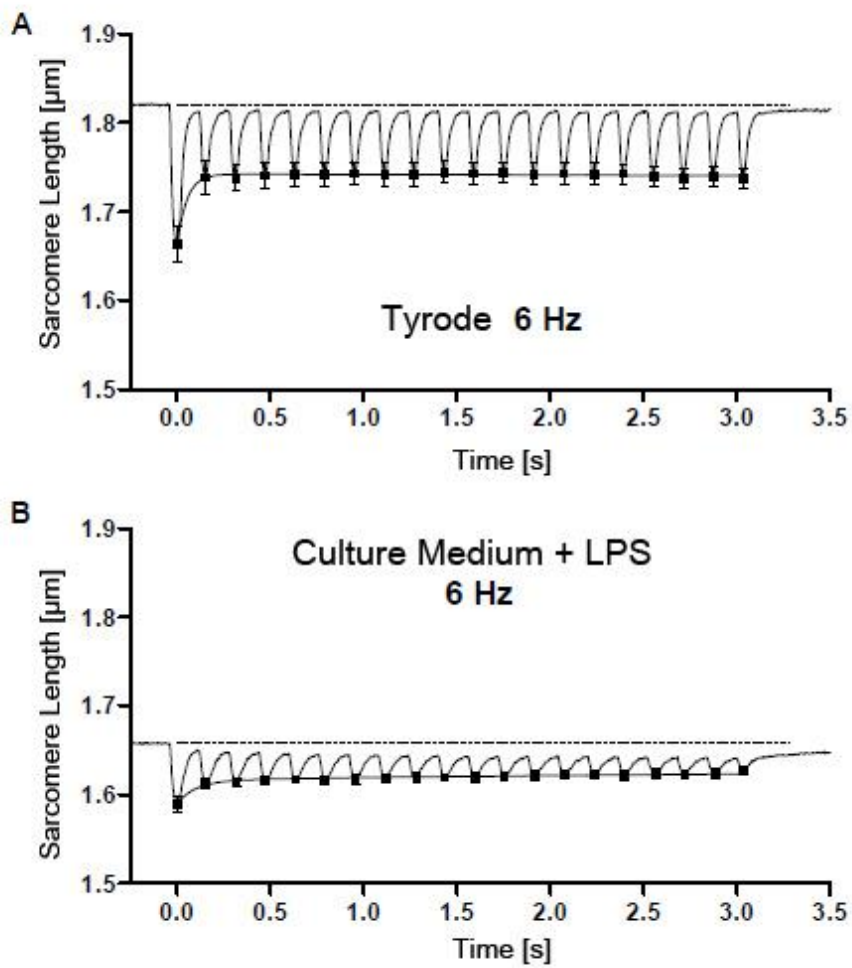


**Fig. 13:** Averaged original registration of sarcomere shortenings of isolated cardiomyocytes of C57BL/6 mice during 20 external stimulations at 6 Hz. (A) shows the average of freshly isolated cells suspended in Tyrode's solution (n=43). (B) shows the average of shortenings of cardiomyocytes incubated in culture medium with LPS for 6 hours (n=11). Standard error is marked. After the post-rest shortening, both groups did not develop a staircase. Standard error is marked.



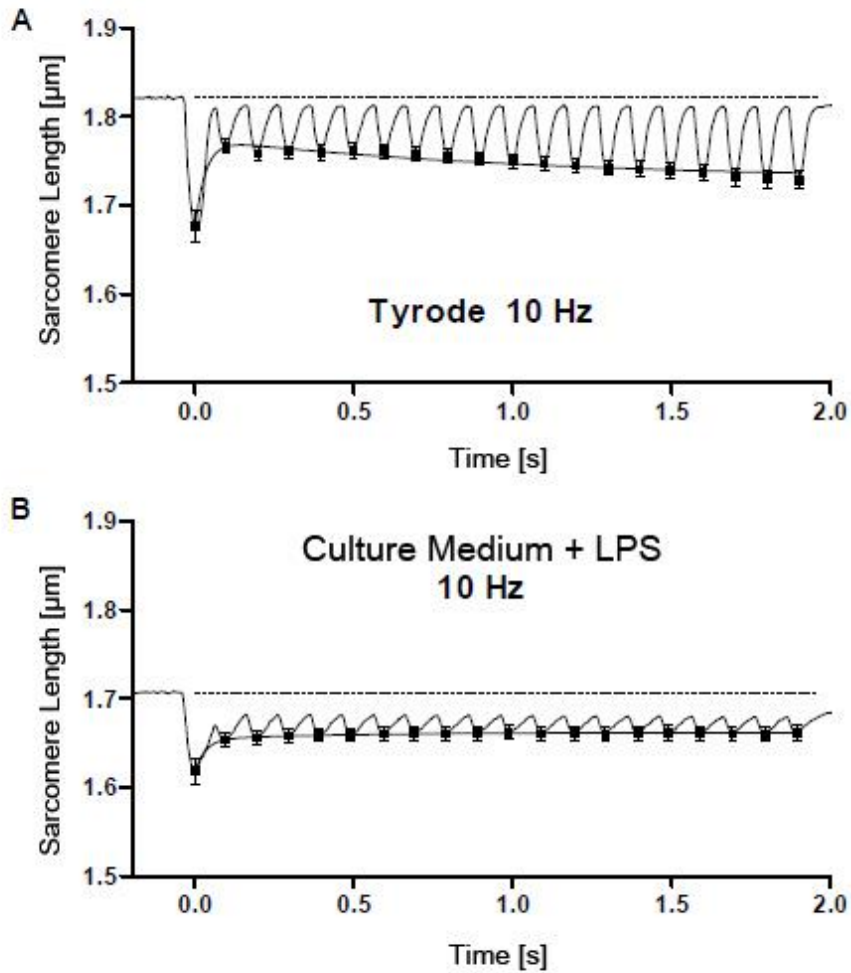


**Fig. 14:** Averaged original registrations of sarcomere shortenings of isolated cardiomyocytes of C57BL/6 mice during 20 external stimulation at 10 Hz. (A) shows the average of freshly isolated cells suspended in Tyrode's solution ( $n=31$ ). (B) shows the average of shortenings of cardiomyocytes incubated in culture medium with LPS for 6 hours ( $n=15$ ). Standard error is marked. The nonlinear regression curve was calculated with the formula 3.1. The group (A) shows a distinct "positive staircase" pattern. Group (B), on the other hand, did not develop a distinct staircase after the post-rest shortening.

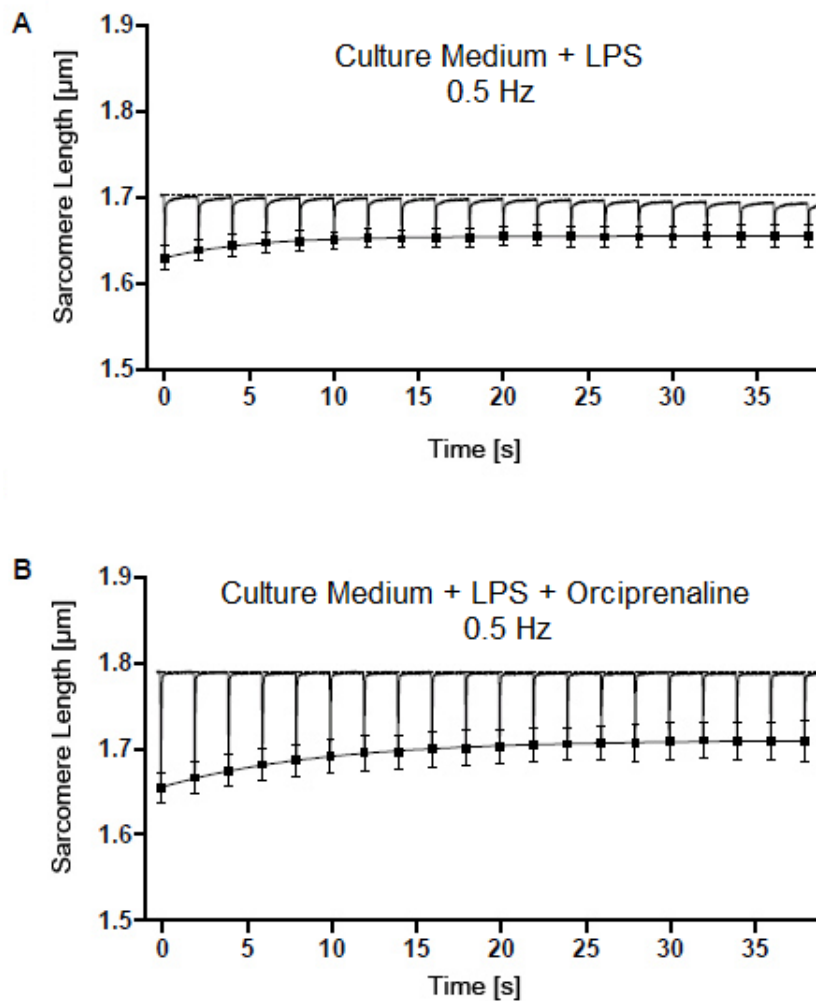


**Fig. 15:** Averaged original registrations of sarcomere shortenings of isolated cardiomyocytes of C57BL/6 mice during 20 external stimulations at 0.5 Hz. (A) shows the average of shortenings of cardiomyocytes incubated in culture medium with LPS for 6 Hours ( $n=18$ ). (B) shows the average of shortenings of cardiomyocytes incubated in culture medium with LPS for 6 hours under  $\beta$ -stimulation with the addition of orciprenaline ( $n=24$ ). Standard error margin is marked. The nonlinear regression curve was calculated with the formula 3.1. For both groups the “negative staircase” pattern can be seen.

### 3.4 Contraction Parameters

The acquired parameters described in 2.3.1 are graphically portrayed below in order to demonstrate the characteristics of cardiomyocyte contraction for each group.

#### 3.4.1 Resting Sarcomere Length, Tyrode vs. Tyrode + Orciprenaline

The sarcomere length at a relaxed state could be measured by the program (IonWizard®) automatically. The addition of orciprenaline in the concentration of 0.3  $\mu\text{g}/\text{ml}$  in Tyrode induced a small shortening of resting sarcomere at all tested frequencies (See Figure 16). However, this was not enough for a statistic significance.

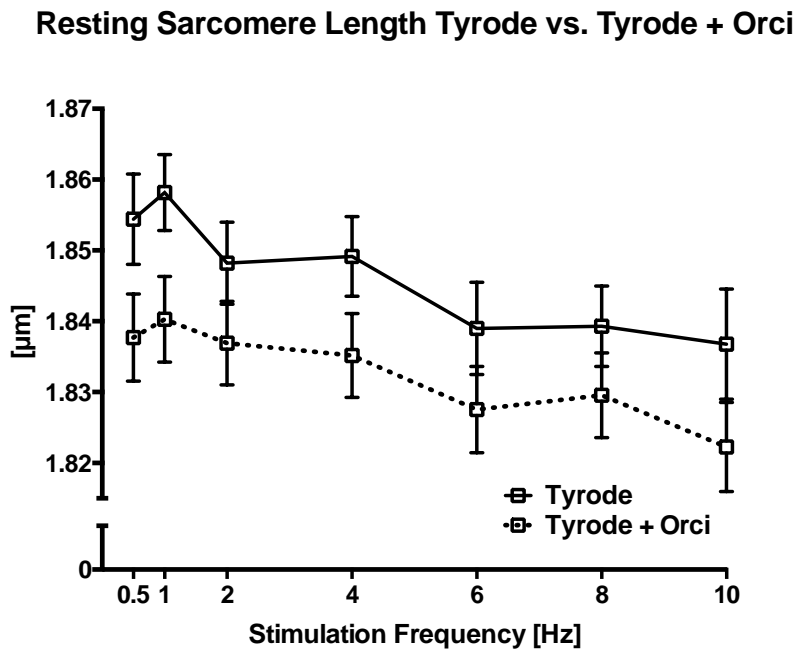


**Fig. 16:** The average resting sarcomere length (in  $\mu\text{m} \pm \text{SEM}$ ) of cardiomyocytes is plotted as function of the stimulation frequency in Hz. Significant differences could not be detected. The numbers of isolated cardiomyocytes used in each group are listed in Supplement 7.2.

### 3.4.1.1 Resting Sarcomere Length, Tyrode vs. Culture Medium + Orciprenaline

The cultured group showed significant shortening of resting sarcomere at all tested frequencies. The incubated cells had a shorter resting sarcomere length compared to the freshly isolated cells suspended in Tyrode's solution. The presence of orciprenaline in the concentration of 0.3  $\mu\text{g}/\text{ml}$  in the cultured group induced a significant shortening of resting sarcomere at all tested frequencies compared to the group without orciprenaline. A significant frequency dependency could not be demonstrated (See Figure 17).

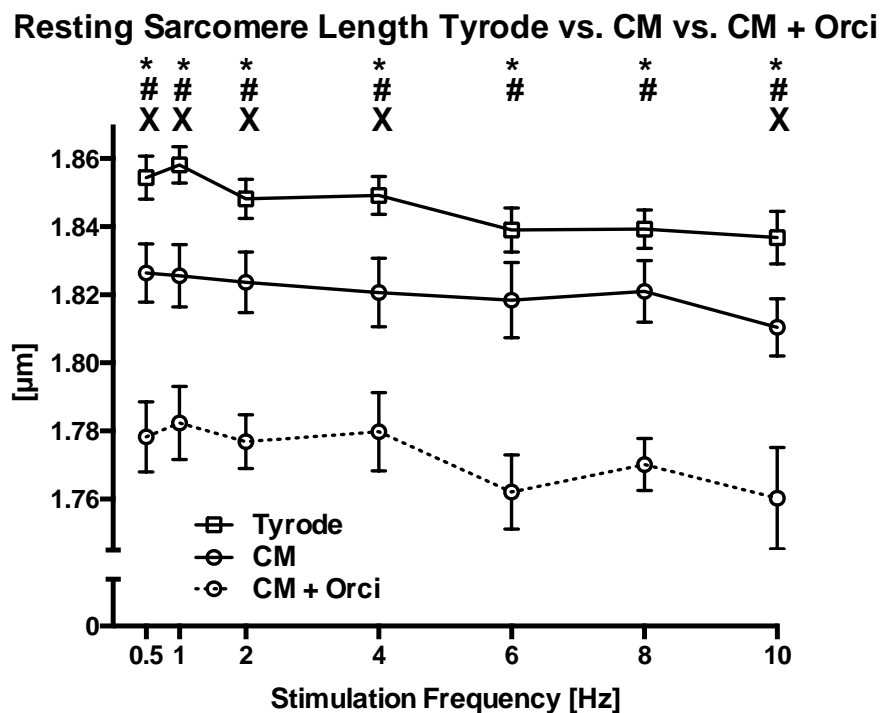


**Fig. 17:** The average resting sarcomere length (in  $\mu\text{m} \pm \text{SEM}$ ) of cardiomyocytes is plotted as function of the stimulation frequency in Hz. (significance \* marked for Tyrode vs. Culture Medium + Orciprenaline; significance # marked for Culture Medium vs. Culture Medium + Orciprenaline; significance x marked for Tyrode vs. Culture Medium) The numbers of isolated cardiomyocytes used in each group are listed in Supplement 7.2.

### 3.4.1.2 Resting Sarcomere Length, Culture Medium + LPS vs. Culture Medium + LPS + Orciprenaline

The presence of LPS in the culture medium had no influence on the resting sarcomere length. After the addition of orciprenaline in the concentration of 0.3  $\mu\text{g/ml}$  in the cultured group with LPS, a small difference in the shortening of the resting sarcomere length was observed, but not enough for a statistical significance (See Figure 18).

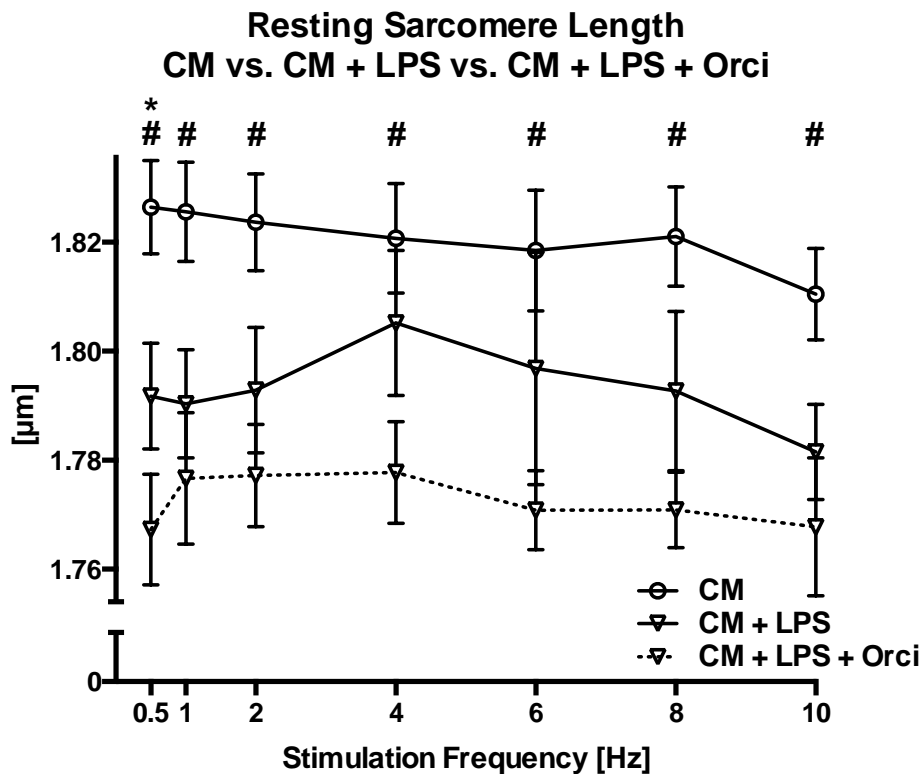


**Fig. 18:** The average resting sarcomere length (in  $\mu\text{m} \pm \text{SEM}$ ) of cardiomyocytes is plotted as function of the stimulation frequency in Hz. (significance \* marked for Culture Medium vs. Culture Medium + LPS; significance # marked for Culture Medium vs. Culture Medium + LPS + Orciprenaline) The numbers of isolated cardiomyocytes used in each group are listed in Supplement 7.2.

### 3.4.2 Sarcomere Shortening Amplitude, Tyrode vs. Tyrode + Orciprenaline

The shortening amplitude was calculated by IonWizard. The program calculated the difference between the resting sarcomere length and the minimum of a shortening curve. The function of shortening amplitude and frequency exhibited a biphasic shape with a local maximum at low stimulation frequencies, a minimum at 2 Hz and a high plateau at stimulation frequencies  $\leq 6$  Hz. The addition of orciprenaline in the concentration of  $0.3 \mu\text{g/ml}$  significantly increased the shortening amplitude of the cells by  $0.1 \mu\text{m} - 0.15 \mu\text{m}$  at all stimulated frequencies. The shortening amplitude rose in the average of  $135.6 \%$  (See Figure 19).

#### Sarcomere Shortening Amplitude Tyrode vs. Tyrode + Orci

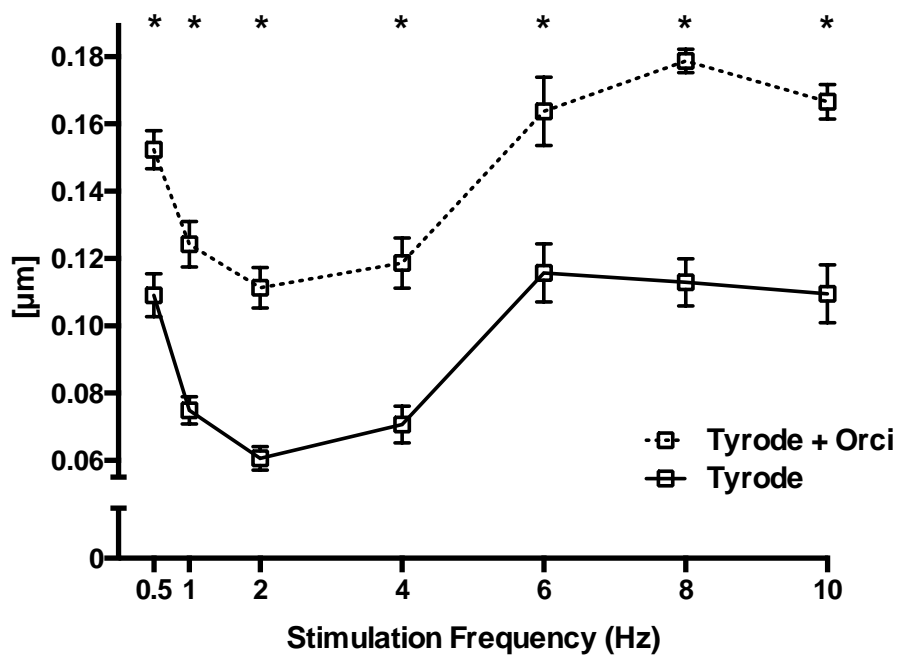


**Fig. 19:** The average sarcomere shortening amplitude (in  $\mu\text{m} \pm \text{SEM}$ ) of cardiomyocytes is plotted as function of the stimulation frequency in Hz. (significance \* marked for Tyrode vs. Tyrode + Orciprenaline) The numbers of isolated cardiomyocytes used in each group are listed in Supplement 7.3.

### 3.4.3 Sarcomere Shortening Speed, Tyrode vs. Tyrode + Orciprenaline

Analogue to the frequency dependence of the shortening amplitude, the shortening speed also showed a biphasic pattern with a minimum around 2 Hz - 4 Hz and the peak at around 6 Hz - 8 Hz (See Figure 20). The addition of orciprenaline in the concentration of 0.3  $\mu\text{g/ml}$  in the freshly isolated Tyrode group induced a significant increase in shortening speed at all tested frequencies. The shortening speed rose in the average of 62.4 %. The biphasic pattern became more apparent as well.

### Sarcomere Shortening Speed Tyrode vs. Tyrode + Orciprenaline

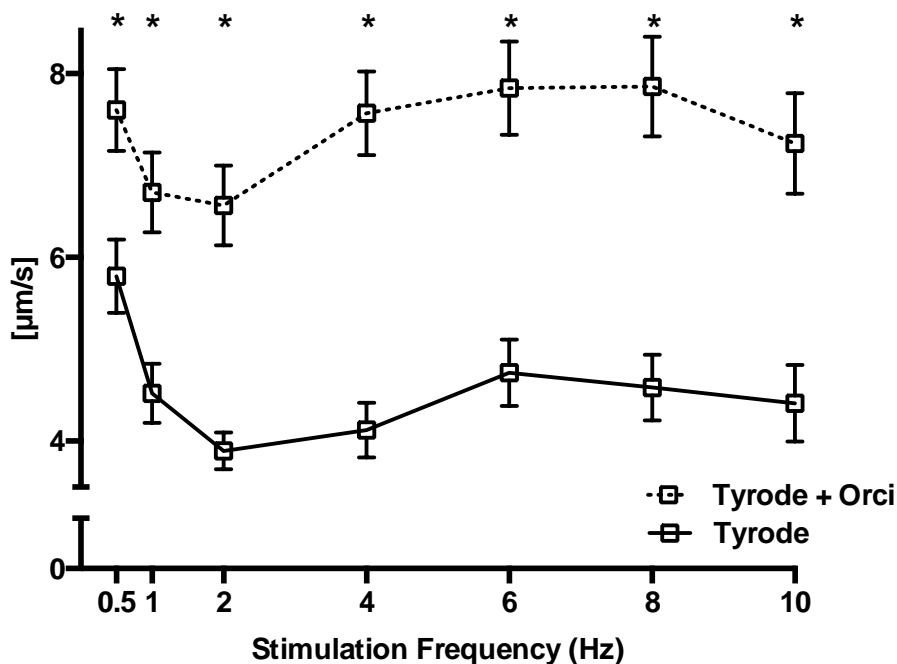


**Fig. 20:** The average sarcomere shortening speed (in  $\mu\text{m/s} \pm \text{SEM}$ ) of cardiomyocytes is plotted as function of the stimulation frequency in Hz. (significance \* marked for Tyrode vs. Tyrode + Orciprenaline) The numbers of isolated cardiomyocytes used in each group are listed in Supplement 7.4.

#### **3.4.4 Sarcomere Relaxation Speed**

Analogue to the shortening speed, the tangential line drawn on the steepest ascending part of a shortening curve was taken as the slope of a given shortening to calculate the relaxation speed. The curves also showed a biphasic pattern with the low point at 2 Hz and the high point at around 6 Hz – 8 Hz while the pattern was not as distinctive as in other parameters. The cells incubated in culture medium had lower relaxation speed than in the freshly isolated Tyrode group.



### 3.4.4.1 Relaxation Speed, Tyrode vs. Tyrode + Orciprenaline

The presence of orciprenaline in the concentration of 0.3  $\mu\text{g/ml}$  induced a significant increase in relaxation speed at all tested frequencies. The relaxation speed rose in the average of 57.8 %. The biphasic pattern became more apparent as well, for example at 8 Hz (See Figure 21).

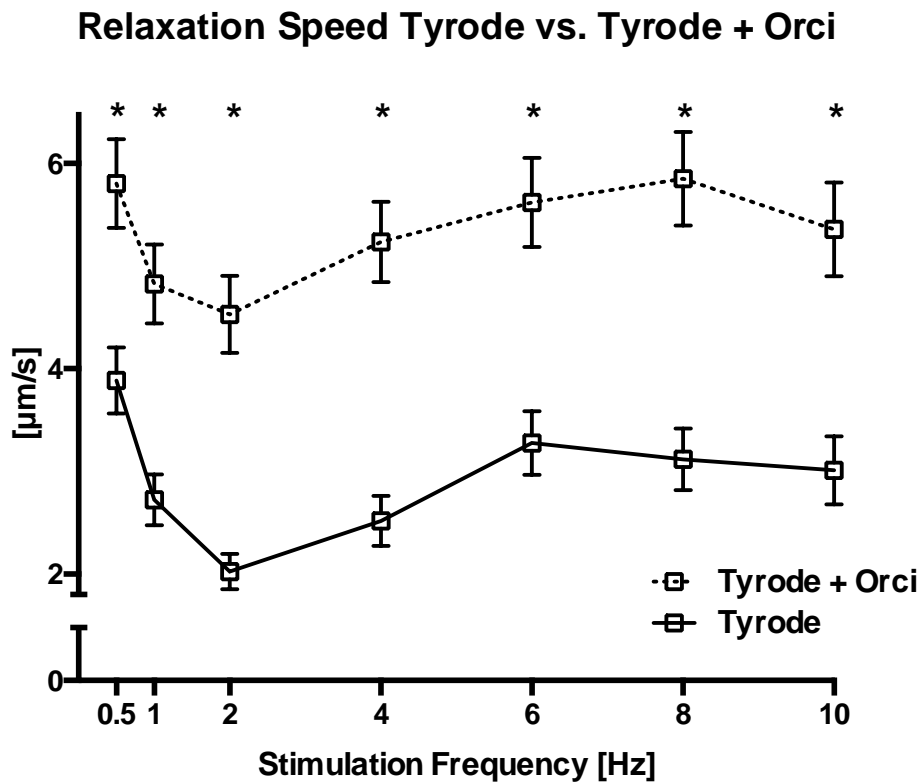


**Fig. 21:** The average relaxation speed (in  $\mu\text{m/s} \pm \text{SEM}$ ) of cardiomyocytes is plotted as function of the stimulation frequency in Hz. (significance \* marked for Tyrode vs. Tyrode + Orciprenaline) The numbers of isolated cardiomyocytes used in each group are listed in Supplement 7.5.

### 3.4.5 Sarcomere Shortening Amplitude in Culture Medium

The incubation of the cells in culture medium for 6 hours reduced the shortening amplitude significantly, which was by 28.7% in average. The addition of orciprenaline in the concentration of 0.3  $\mu\text{g/ml}$  to the culture medium increased the shortening amplitude significantly at all stimulation frequencies. Under these conditions the shortening amplitude significantly exceeded that of freshly isolated cells in Tyrode's solution. The stimulating effect of orciprenaline in culture medium amounted to 97.5 % in average (See Figure 22).

**Sarcomere Shortening Amplitude Tyrode vs. CM vs. CM + Orci**

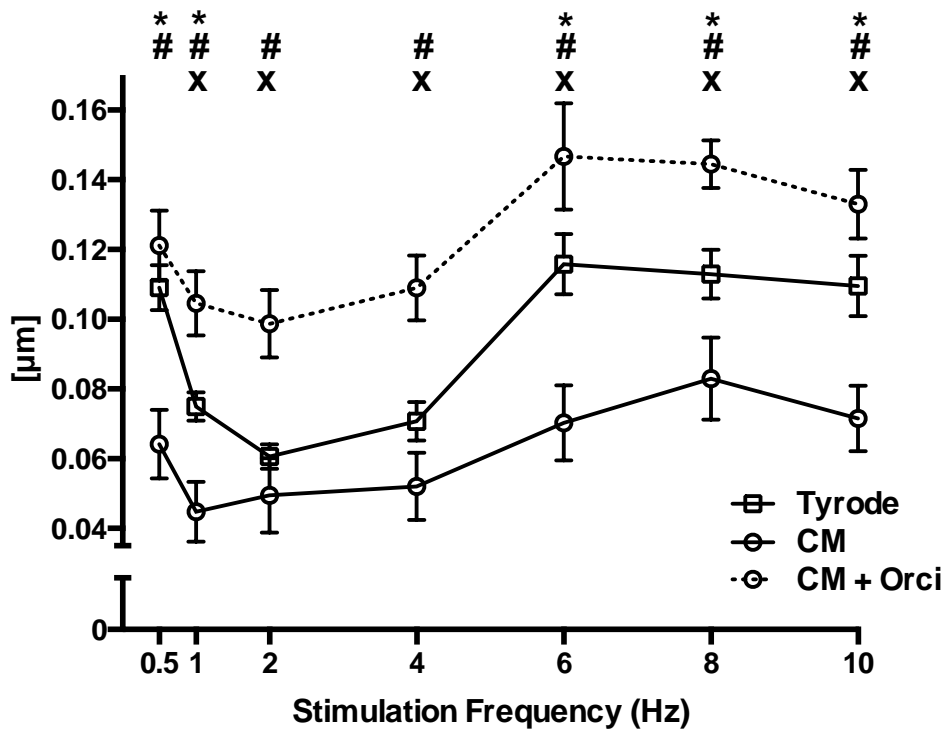


**Fig. 22:** The average sarcomere shortening amplitude (in  $\mu\text{m} \pm \text{SEM}$ ) of cardiomyocytes is plotted as function of the stimulation frequency in Hz. (significance marked \* for Tyrode vs. Culture Medium; significance # marked for Culture Medium vs. Culture Medium + Orciprenaline; significance x marked for Tyrode vs. Culture Medium + Orciprenaline) The numbers of isolated cardiomyocytes used in each group are listed in Supplement 7.3.

### 3.4.5.1 Sarcomere Shortening Amplitude, Tyrode + Orciprenaline vs. Culture Medium + Orciprenaline

When the shortening amplitude of freshly isolated cells with orciprenaline was compared with the shortening amplitude of incubated cells with orciprenaline, there were some significant differences, but not at all frequencies. The level reached in culture medium with orciprenaline remained still below that of freshly isolated cells in Tyrode solution with orciprenaline (See Figure 23).

#### Sarcomere Shortening Amplitude Tyrode + Orcki vs. CM + Orcki

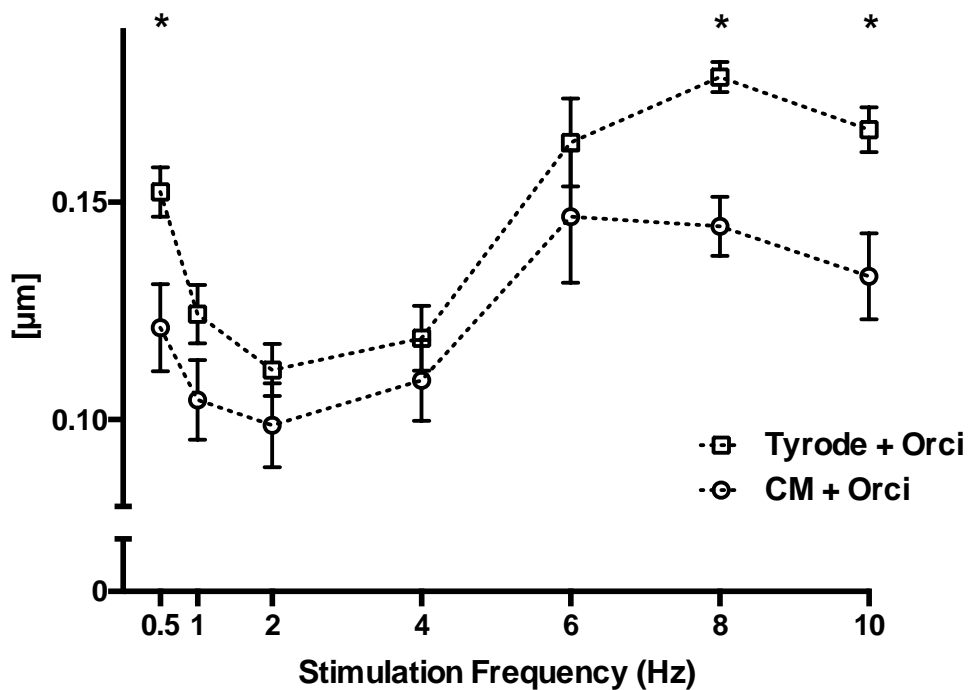


**Fig. 23:** The average sarcomere shortening amplitude (in  $\mu\text{m} \pm \text{SEM}$ ) of cardiomyocytes is plotted as function of the stimulation frequency in Hz. (significance marked \* for Tyrode + Orciprenaline vs. Culture Medium + Orciprenaline) The numbers of isolated cardiomyocytes used in each group are listed in Supplement 7.3.

### 3.4.6 Sarcomere Shortening Speed, Culture Medium + Orciprenaline vs. Tyrode vs. Culture Medium

The incubation of the cells in culture medium for 6 hours reduced the shortening speed significantly. The addition of orciprenaline in the concentration of 0.3  $\mu\text{g/ml}$  to the culture medium increased the shortening speed significantly at most stimulation frequencies. Under these conditions the shortening speed significantly exceeded that of freshly isolated cells in Tyrode's solution. The stimulating effect of orciprenaline in culture medium amounted to 82.3 % in average (See Figure 24).

**Sarcomere Shortening Speed CM + Orcki vs. Tyrode vs. CM**

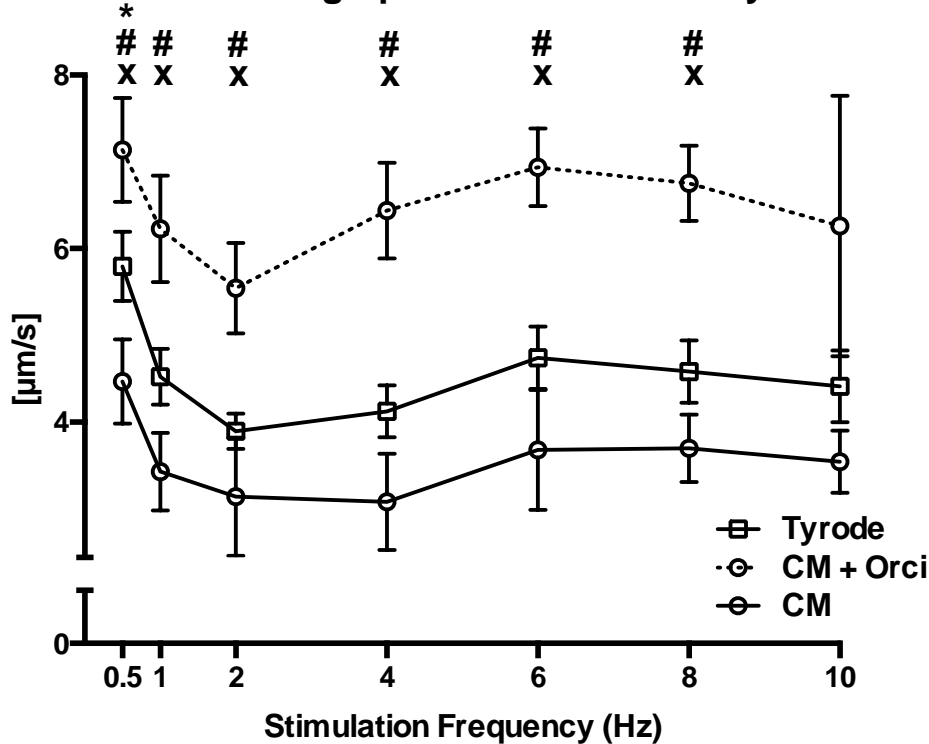


**Fig. 24:** The average sarcomere shortening speed (in  $\mu\text{m/s} \pm \text{SEM}$ ) of cardiomyocytes is plotted as function of the stimulation frequency in Hz. (significance marked \* for Tyrode vs. Culture Medium; significance marked # for Culture Medium vs. Culture Medium + Orciprenaline; significance marked x for Tyrode vs. Culture Medium + Orciprenaline) The numbers of isolated cardiomyocytes used in each group are listed in Supplement 7.4.

### 3.4.7 Relaxation Speed, Tyrode vs. Culture Medium vs. Culture Medium + Orciprenaline

Similarly, the incubation of the cells in culture medium for 6 hours reduced the relaxation speed significantly in many stimulation frequencies. The addition of orciprenaline in the concentration of 0.3  $\mu\text{g/ml}$  to the culture medium increased the relaxation speed significantly at all frequencies, in the average of 276.8 %. Under these conditions the relaxation speed significantly exceeded that of freshly isolated cells in Tyrode solution (See Figure 25).

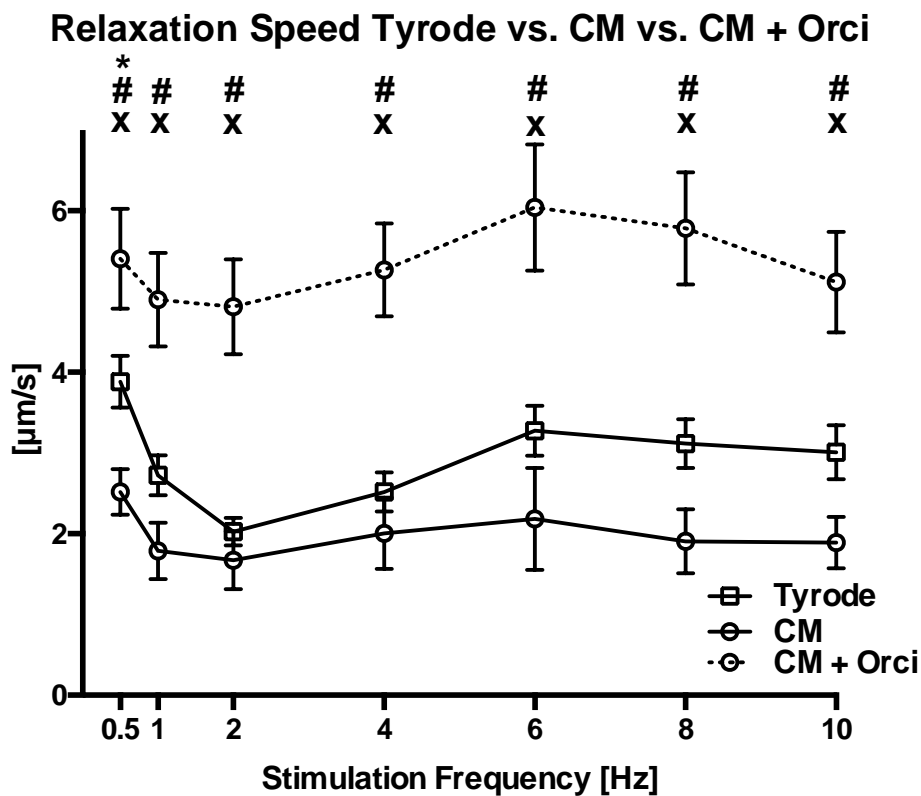


**Fig. 25:** The average relaxation speed (in  $\mu\text{m/s} \pm \text{SEM}$ ) of cardiomyocytes is plotted as function of the stimulation frequency in Hz. (significance marked \* for Tyrode vs. Culture Medium; significance marked # for Culture Medium vs. Culture Medium + Orciprenaline; significance marked x for Tyrode vs. Culture Medium + Orciprenaline) The numbers of isolated cardiomyocytes used in each group are listed in Supplement 7.5.

### 3.4.8 Sarcomere Shortening Amplitude, Culture Medium vs. Culture Medium + LPS vs. Culture Medium + LPS + Orciprenaline

Addition of orciprenaline elevated the shortening amplitude in the Culture Medium + LPS + Orciprenaline group at all tested frequencies compared to Culture Medium + LPS group. Addition of orciprenaline elevated the shortening amplitude in the Culture Medium + LPS + Orciprenaline group even above the Culture Medium control group. Level of significance was reached at the frequencies 0.5, 1, 2, 6, 8 and 10 Hz. The shortening amplitude rose here in the average by 124.9 %. The negative effect of LPS on shortening amplitude of incubated cells could be demonstrated significantly only at 8 Hz (See Figure 26).

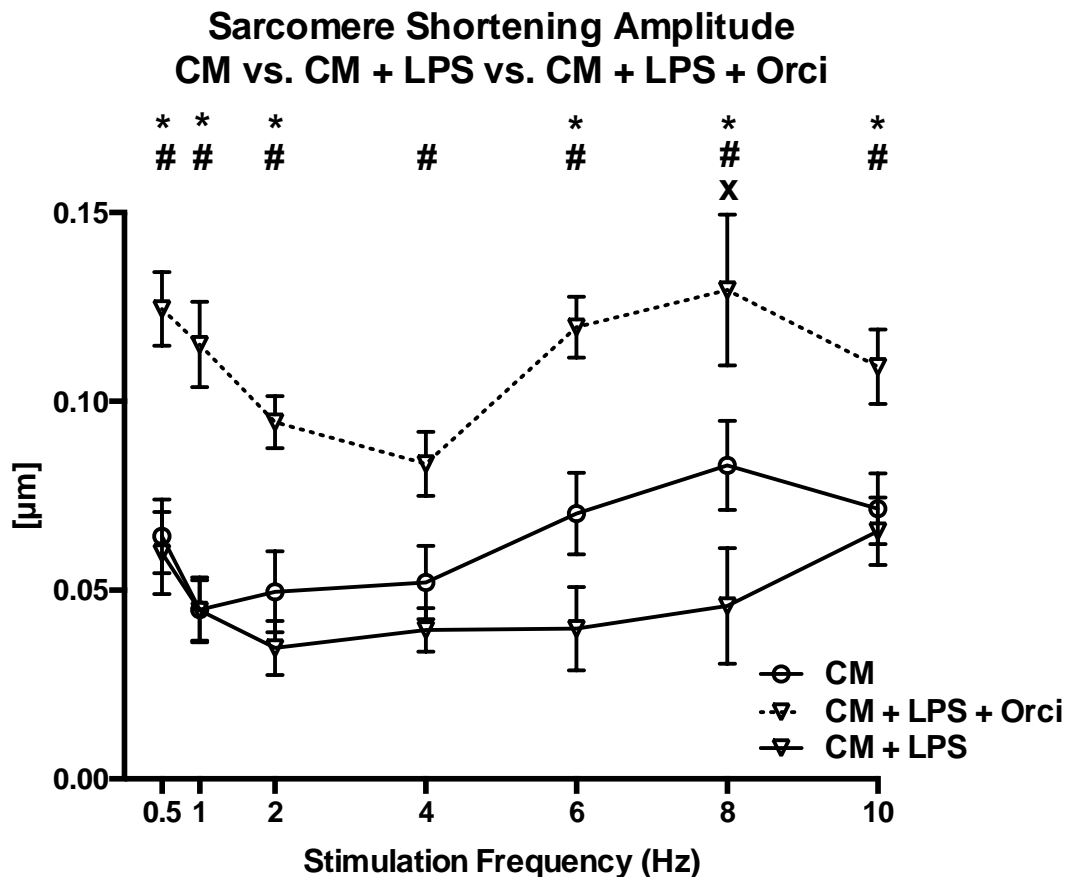


**Fig. 26:** The average sarcomere shortening amplitude (in  $\mu\text{m} \pm \text{SEM}$ ) of cardiomyocytes is plotted as function of the stimulation frequency in Hz. (significance marked \* for Culture Medium + LPS vs. Culture Medium + LPS + Orciprenaline; significance marked # for Culture Medium vs. Culture Medium + LPS + Orciprenaline; significance marked x for Culture Medium vs. Culture Medium + LPS) The numbers of isolated cardiomyocytes used in each group are listed in Supplement 7.3.

### 3.4.9 Sarcomere Shortening Amplitude, Culture Medium + Orciprenaline vs. Culture Medium + LPS + Orciprenaline

The addition of orciprenaline in the concentration of 0.3  $\mu\text{g/ml}$  induced a significant increase in shortening amplitude in the Culture Medium + Orciprenaline group (Culture Medium vs. Culture Medium + Orciprenaline) at all frequencies and in the Culture Medium + LPS + Orciprenaline group (Culture Medium vs. Culture Medium + LPS + Orciprenaline) in the frequencies 0.5, 1, 2, 6, and 8 Hz. The effect of orciprenaline in both incubated groups was so prominent, that there wasn't a significant difference in the shortening amplitude in any frequency between Culture Medium + Orciprenaline group and Culture Medium + LPS + Orciprenaline group (See Figure 27).

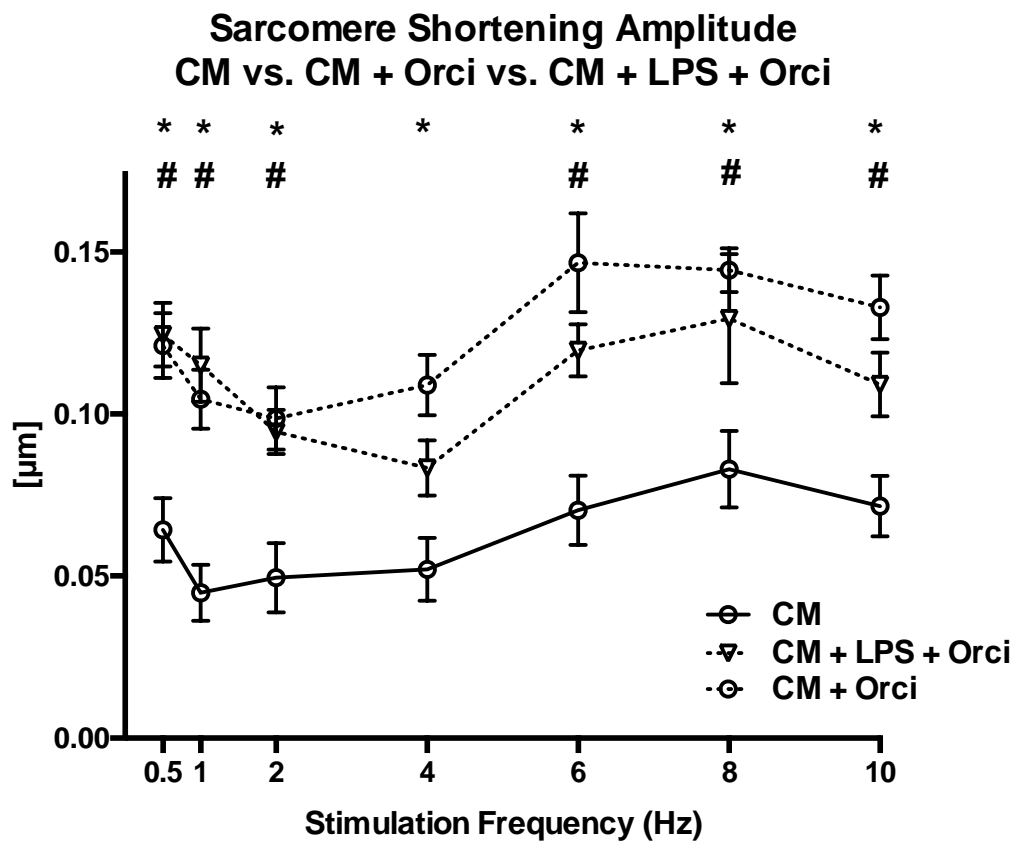


**Fig. 27:** The average sarcomere shortening amplitude (in  $\mu\text{m} \pm \text{SEM}$ ) of cardiomyocytes is plotted as function of the stimulation frequency in Hz. (significance marked \* for Culture Medium vs. Culture Medium + Orciprenaline; significance marked # for Culture Medium vs. Culture Medium + LPS + Orciprenaline) The numbers of isolated cardiomyocytes used in each group are listed in Supplement 7.3.

### 3.4.10 Sarcomere Shortening Speed, Culture Medium vs. Culture Medium + LPS vs. Culture Medium + LPS + Orciprenaline

The addition of orciprenaline in the incubated group with LPS in the concentration of 0.3  $\mu\text{g}/\text{ml}$  induced a significant increase in shortening speed at all tested frequencies (Culture Medium + LPS vs. Culture Medium + LPS + Orciprenaline). The shortening speed rose here in the average of 175.9 %. There was a significant difference in the shortening speed between Culture Medium group and Culture Medium + LPS + Orciprenaline group at the frequencies 0.5, 1, 2 and 4 Hz. The effect of LPS on the shortening speed of incubated cells could be demonstrated significantly only at 0.5 Hz (See Figure 28).

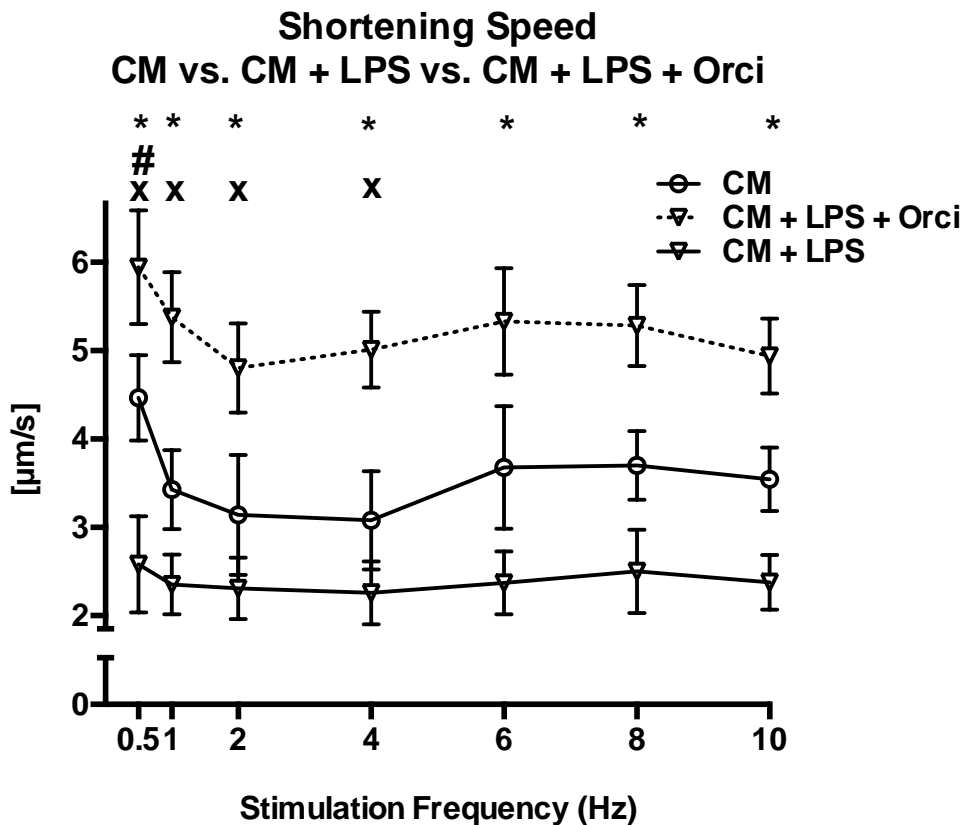


**Fig. 28.:** The average sarcomere shortening speed (in  $\mu\text{m}/\text{s} \pm \text{SEM}$ ) of cardiomyocytes is plotted as function of the stimulation frequency in Hz. (significance marked \* for Culture Medium + LPS vs. Culture Medium + LPS + Orciprenaline; significance marked # for Culture Medium vs. Culture Medium + LPS; significance marked x for Culture Medium vs. Culture Medium + LPS + Orciprenaline) The numbers of isolated cardiomyocytes used in each group are listed in Supplement 7.4.



### 3.4.11 Sarcomere Shortening Speed, Culture Medium + Orciprenaline vs. Culture Medium + LPS + Orciprenaline

After the addition of orciprenaline in all incubated groups in the concentration of 0.3  $\mu\text{g/ml}$ , a tendency of increase in in shortening speed could be observed. However, there was no statistically significant difference between Culture Medium + Orciprenaline group and Culture Medium + LPS + Orciprenaline group (See Figure 29).

#### Sarcomere Shortening Speed CM + Orcki vs. CM + LPS + Orcki

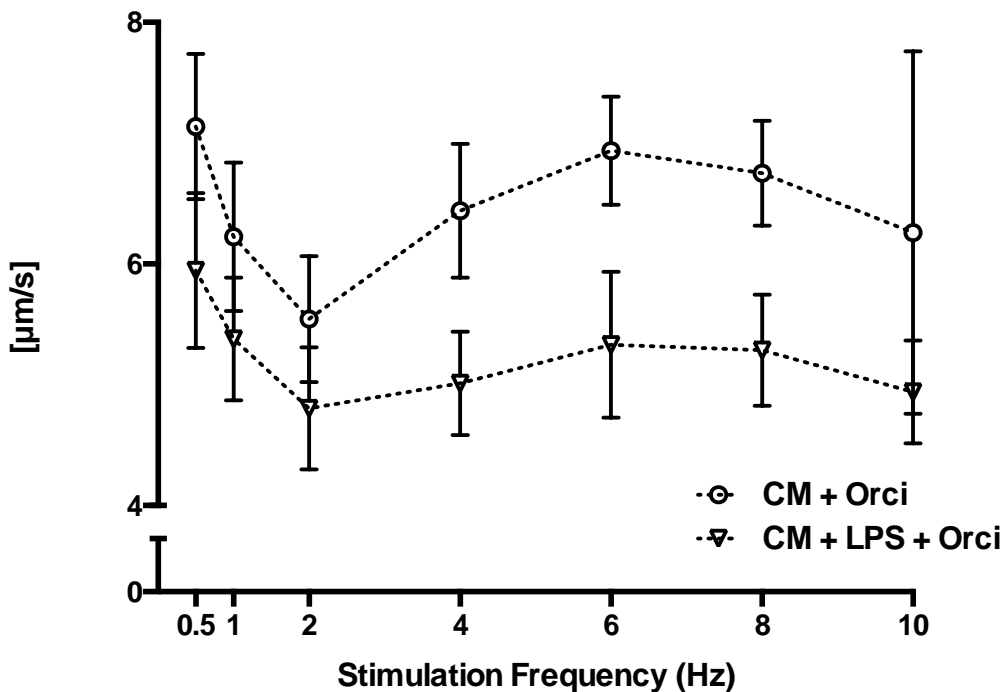


**Fig. 29.:** The sarcomere shortening speed (in  $\mu\text{m/s}$ ) of cardiomyocytes is plotted as function of the stimulation frequency in Hz with average  $\pm$  standard error. There was no significant difference in shortening speed between Culture Medium + Orciprenaline group and Culture Medium + LPS + Orciprenaline group. The numbers of isolated cardiomyocytes used in each group are listed in Supplement 7.4.

### 3.4.12 Sarcomere Relaxation Speed, Culture Medium vs. Culture Medium + LPS vs. Culture Medium + LPS + Orciprenaline

The addition of orciprenaline in Culture Medium + LPS + Orciprenaline group in the concentration of 0.3  $\mu\text{g/ml}$  induced a significant increase in relaxation speed at the frequencies 0.5, 1, 2, 4, and 6 Hz, in the average of 131.6 % when compared to Culture Medium + LPS group. Culture Medium + LPS + Orciprenaline group also showed a significant increase of the relaxation speed when compared to Culture Medium group at the frequencies 0.5, 1, 6 and 8 Hz. The negative effect of LPS on shortening amplitude of incubated cells could not be demonstrated significantly at all frequencies (See Figure 30).

**Relaxation Speed CM vs. CM + LPS vs. CM + LPS + Orcki**

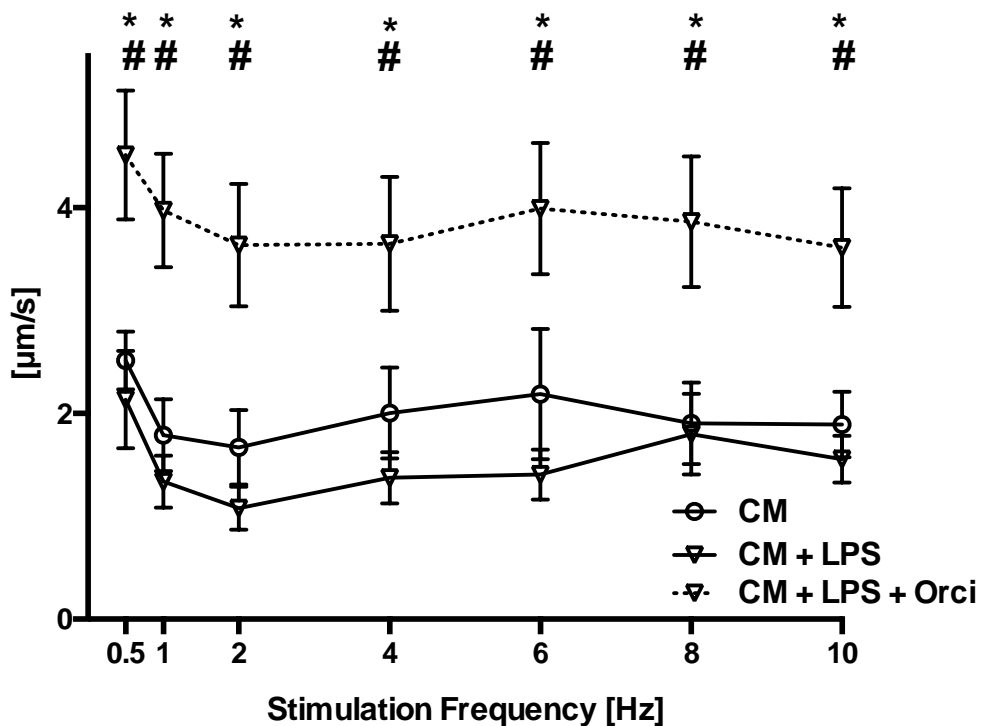


**Fig. 30.:** The average relaxation speed (in  $\mu\text{m/s} \pm \text{SEM}$ ) of cardiomyocytes is plotted as function of the stimulation frequency in Hz. (significance marked \* for Culture Medium + LPS + Orciprenaline vs. Culture Medium + LPS; significance marked # for Culture Medium vs. Culture Medium + LPS + Orciprenaline) There was no significant difference between Culture Medium and Culture Medium + LPS group. The numbers of isolated cardiomyocytes used in each group are listed in Supplement 7.5.

## 4 Discussion

The advancement of modern medicine has brought about many possibilities in treating patients with sepsis. Still, septic cardiomyopathy remains to be a major cause of death in patients suffering from the complications of sepsis and septic shock. About 45% of all patients with diagnosed septicemia develop an acute septic cardiomyopathy, which has a mortality rate up to 70% (Charpentier et al., 2004; Schuster and Müller-Werdan, 2000). The object of this study was to observe the influence of LPS on the shortening of isolated cardiomyocytes *in vitro*, simulating a septic cardiomyopathy. Furthermore, the influence of orciprenaline, a  $\beta$ -stimulation agent, on the shortening of septic cardiomyocytes was observed and the result was compared to the control group.

### 4.1 Validity of the Method

In order to rate the validity of the methods applied in this study it is necessary to evaluate the quality and the reliability of the cell isolation and measuring methods. The techniques used in this study were repeatedly and successfully adopted in many different studies done by our group on various species of animals such as guinea pig, rat, rabbit and mouse (Linz and Meyer, 2000; Meyer, 1989; Tiemann et al., 2003). In mouse, different genotypes were tested (Baumgarten et al., 2006; Kempelmann, 2005; Tiemann et al., 2003; Vervölgyi, 2007). The results of the cell isolation in this study were consistently acceptable. Quantitatively, about 70% of all cells isolated were vital and usable. Qualitatively, most of the vital cells showed the characteristics of healthy cardiomyocytes (rod-shaped, intact cell poles and regular distribution of sarcomere bands). In order to preserve qualities of the isolated cells for 6 hours under various conditions (e.g. stimulation with LPS), the cells were incubated in a culture medium. This specific mixture of four main ingredients (See 2.2.2.1) is based on the description of long term incubating culture medium for isolated cardiomyocytes (Clark et al., 1998; He et al., 1996) and has been successfully and reliably applied by our study group (Baumgarten et al., 2006; Knuefermann et al., 2008; Lohner et al., 2013). However, the resting sarcomere length of all incubated cells was significantly and evenly reduced compared to the freshly isolated cells. This was a predictable phenomenon, already described in

previous studies (Baumgarten et al., 2006; Vervölgyi, 2007). Even though culture medium was applied to stabilize the quality of the cardiomyocytes, their shortening amplitude was significantly reduced compared to the freshly isolated cells in Tyrode's solution (Fig. 22).

The electrical stimulation pattern of 7 different frequencies was chosen for the following reasons. First of all, there should be a 30 second pause between every pulse train, so that the cells were in a comparable state before each stimulation train. The alternating pattern of low and high frequencies (in the order of 0.5, 10, 1, 8, 2, 6 and 4 Hz) was designed to eliminate any influence of high or low frequency stimulation on the next pulse train. The highest frequency in a pulse train was 10 Hz, which was already used by Tiemann et al. (2003). They were able to measure a physiological heart rate of up to  $580 \pm 11/\text{min}$ . in living mice under control conditions. This is an equivalent of about 9.6 Hz. Therefore, a shortening frequency of 10 Hz has to be regarded as physiological in murine cardiomyocytes. It should be noted that only a cell of a good quality can survive an electrical stimulation at 10 Hz, especially when it has already been exposed to stress situations, such as enzymatic isolation, incubation and additional exposure to pathogenic agents like LPS. A stimulation of a cell not fulfilling the criteria of the above described quality (for example, shape, size and sarcomere structure) often resulted in necrosis of the given cell during the stimulation. The majority of publications concerning similar experimental methods did not demonstrate stimulation at high frequencies such as 8 Hz and 10 Hz which speaks for the good quality of the cells used in our study group. Furthermore, the absolute sarcomere length was optically measured and was used for the parameters in this study. This method is independent of the cell size and provides a crucial advantage over the often used "edge detection" technique where the shifting of the cell edge represents the degree of cell shortening. Since the cell size of murine cardiomyocytes varies, the edge detection method requires the normalization of the shortening amplitude to the cell length. This additional step could be omitted by using the sarcomere length measurement.

The LPS concentration used for the incubation (10  $\mu\text{g}/\text{ml}$ ) was chosen because it could be shown in the past (Kinugawa et al., 1997; Wagner et al., 1998) that the LPS-stimulation of murine cardiomyocytes at this concentration had a noticeably depressive effect on the cells without causing a necrosis, therefore simulating a sepsis caused by

gram-negative bacteria. Since then, this concentration has been used in our study group repeatedly (Baumgarten et al., 2006; Vervölgyi, 2007). In order to avoid a possible contamination by LPS already during the isolation process through the use of collagenase isolated from the gram-negative bacterium *Clostridium histolyticum* (See 2.2.1), the collagenase solution was mixed with Polymyxin B, a peptide-antibiotic substance which binds free LPS particles, depressing its toxicity (Warner et al., 1985).

The time frame in which the incubated cells could be stimulated and measured was 5 to 8 hours after the isolation. This was based on earlier results of Baumgarten et al. (2006) which showed that the maximum negative influence of LPS on cell shortening was detected after 5 hours of incubation. Therefore, an incubation time of 6 hours was chosen in this study so that a maximum effect of LPS was expected and there were still 2 hours remaining for the measurements.

#### **4.2 The effects of orciprenaline on the shortening of cardiomyocytes**

Since the description of the positive chronotropic effect of epinephrine in the 1940s (Barcroft et al., 1949), the positive effect of catecholamine on the contractility of the heart, even on the molecular level, has been researched often and understood in detail (Review: Mann, 2015; Shanks et al., 1967). In our study, it has also been shown that the addition of the  $\beta_1$  agonist orciprenaline at the concentration of 0.3  $\mu\text{g}/\text{ml}$  resulted in a significant improvement of the shortening in all cell groups to which it had been added (Tyrode, Culture Medium, Culture Medium + LPS). This result correlated to a previous study of our group (Weisser-Thomas et al., 2015). In their study, orciprenaline induced a significant concentration-dependent positive inotropic effect in myocytes of wildtype mice, causing a rise of sarcomere shortening by 161.2% in Tyrode at 0.5 Hz at the orciprenaline concentration of 0.25  $\mu\text{g}/\text{ml}$  vs. 0.3  $\mu\text{g}/\text{ml}$  here. At 0.5 Hz, e.g., the addition of orciprenaline caused an elevation of shortening amplitude in the Tyrode group by 142.3 %. Culture Medium group showed an elevation of shortening amplitude by 182.5 % at 0.5 Hz. Thus, the results of the present study confirmed the previous results of our study group. This further underlines that the cells used in this study were in good physical condition.

### 4.3 Signal Cascade from TLR4 to Cardiac Depression in the Presence of Lipopolysaccharide

The reduction of cardiac contractility in the form of a septic cardiomyopathy is a frequent and serious complication of a severe sepsis. Since the isolation of Lipopolysaccharide in 1943 (Shear and Turner, 1943), it has been shown that LPS is an essential component of the outer cell membrane of the most gram-negative bacteria and one of the strongest known immune stimulating substances (Alexander and Rietschel, 2001).

In a preceding study, Baumgarten et al. (2006) demonstrated that 10µg/ml LPS applied to isolated cardiomyocytes of CH3/HeN mice was able to suppress the sarcomere shortening via the TLR4 pathway. This suppression of sarcomere shortening could be prevented by application of the TLR4 antagonist Eritoran or by application of SMT (S-methylisothiourrea), an iNOS blocker. This showed that iNOS and NO are involved in the TLR4 dependent decrease of cardiac sarcomere shortening.

Ullrich et al. (2000) could show that iNOS deficient mice (chromosome 17) did not show any relevant cardiac depression after having been exposed to bacterial endotoxin. Furthermore, Vervölgyi (2007) of our study group showed that LPS also affected the contractility of cardiomyocytes by reducing the calcium sensitivity. This finding was supported by earlier results of Rastaldo et al. (2007) and Massion and Balligand (2003) who demonstrated that high concentrations of nitric oxide (NO) impair cardiac function through activation of protein kinase G followed by Ca<sup>2+</sup> desensitization of troponin (Ehrentraut et al., 2011).

In addition, it was demonstrated that block of iNOS by SMT was also able to restore the reduced sarcomere shortening after TLR9 stimulation (Knuefermann et al., 2008).

In the present study, LPS also significantly depressed sarcomere shortening amplitude as well as shortening and relaxation speed of C57BL/6 cardiomyocytes. Although sarcomere shortening amplitude was significantly reduced only at 8 Hz stimulation frequency, also the values of 4 and 6 Hz were lower than those of control and the shape of the graph had changed completely. However, in this study, the depressive effect of LPS on the shortening of the C57BL/6 cardiomyocytes was less prominent than in the cardiomyocytes isolated from C3H/HeN mice.

There are four possible explanations for this phenomenon. First, the LPS used in this

study (Sigma-Aldrich, St. Louis, MO, USA, L-3024, see 2.2.2.2) could have had a different virulence, because the Lipid A-component of LPS may vary, depending on the type of bacterium from which it has been isolated. This possibility, however, could be eliminated because here the same LPS from Sigma-Aldrich, isolated from the bacterium *Escherichia coli*-Serotype O111:B4 was applied as in all our previous studies.

The second possible explanation is that the cells became insensitive to LPS due to an early exposure to LPS already during the isolation process because of a possible contamination of the collagenase which was isolated from *Clostridium histolyticum*. However, as mentioned in 4.1, the use of Polymyxin B in the isolation process should bind free LPS particles, inactivating the possible toxicity. This method had also been applied in our previous studies, therefore we think that lower LPS sensitivity by pre-exposure of the cells is not plausible.

The third explanation is that the phenomenon could be attributed to the different strain of mice investigated. The strain of mice used in this study (C57BL/6) may have been less sensitive to LPS in comparison to the mouse type C3H, which was used in our previous studies (Ehrentraut et al., 2011; Vervölgyi, 2007). It has been observed by other study groups that C57BL/6 mice were less sensitive to the stimulus of LPS than BALB/c mice (Oliveira et al., 2014, Santos et al., 2006).

The fourth, and the most likely, explanation is that the Culture Medium group had a smaller shortening amplitude than was detected previously (Baumgarten et al., 2006). This resulted in a smaller signal to noise ratio in the Culture Medium + LPS group. Furthermore, the observation that LPS application also significantly reduced the shortening speed at low stimulation frequencies underlines that LPS had a clear negative inotropic effect on the C57BL/6 cardiomyocytes.

#### **4.4 “Rescue Effect” of Orciprenaline in the Presence of LPS**

As shown in 4.3, the incubation with LPS caused a significant depression of sarcomere shortening. After addition of orciprenaline to the LPS incubated group, the sarcomere shortening not only recovered but even significantly exceeded that of the control group. This positive, “rescue effect” due to orciprenaline on the sarcomere shortening was so prominent, that the shortening amplitudes reached the same level as those after

orciprenaline without LPS pre-treatment (See Figure 27). Thus,  $\beta$ -stimulation seems to be sufficient to overcome the negative inotropic influences of LPS. However, it is well known that the effect of  $\beta$ -stimulation does not last for a long time because of  $\beta$  receptor desensitization (Freedman et al., 1995). In this study, it could be shown that LPS stimulation can be completely overcome by beta stimulation in single isolated cardiomyocytes. I.e. the antagonistic effect of LPS and beta stimulation act on the single cell level in the heart.  $\beta$ -stimulation was able to rule out the LPS effect completely on the same cell. Thus, the aim of this study to quantitatively characterize the influence of  $\beta$ -stimulation and LPS intoxication on single cells can be considered as met.

#### **4.5 Conclusion**

In this study, the negative effect of LPS on sarcomere shortening was demonstrated. It was also shown that the addition of orciprenaline could compensate for the depressive effect of LPS fully. Interestingly, LPS pre-treated cells reacted so strong to  $\beta$ -stimulation, that they were able to shorten with same amplitude as the control group after  $\beta$ -stimulation.

As mentioned in the introduction, septicemia and septic shock are responsible for many complications leading to most deaths in Intensive Care Unit (ICU) patients. A bacterial septicemia can lead to septic cardiomyopathy and septic vascular leakage, which then causes a circulation failure and eventually the death of a patient (Ramirez et al., 2017). Therefore, the question whether or not to initiate a catecholamine therapy in a septic patient possesses a high clinical relevance. In every day ICU setting, the catecholamine therapy is readily applied to a septic patient in order to sustain the blood pressure of the patient, which is an indisputable priority. This study proved that the above mentioned “rescue effect” of a  $\beta$ -stimulation was able to completely reverse the negative influence of LPS on shortening even on the level of isolated cardiomyocytes. This may, in part, explain the benefit of the catecholamine therapy in patients. Furthermore, in patients, this therapy does not only improve myocardial contractility and ejection fraction of the heart in the whole, but also has a vasocontractile effect through the stimulation of  $\alpha$ -receptors. The combination of these two effects can be expected to lead to a more positive effect on the blood pressure of the patient in the medication-based circulation



management. The present study was able to extend a clinically proven therapy of septic cardiomyopathy to the level of single cardiomyocytes.

## 5 Zusammenfassung

Die septische Kardiomyopathie geht mit einer hohen Morbidität und Mortalität einher. In der Sepsis wird die Kontraktilität der einzelnen Kardiomyozyten stark vermindert. Die Pumpleistung des Herzens als Gesamtorgan reduziert sich somit massiv. Etwa ein Fünftel aller septischen Patienten sterben aufgrund des herabgesetzten kardialen Auswurfs (Engl. „low cardiac output syndrome“) unter septischer Kardiomyopathie. Ein solcher intensivpflichtige Patient bedarf in der Regel einer prolongierten hochdosierten Katecholamintherapie. In dieser Studie wurde der Einfluss von Katecholaminen auf die Kontraktilität einzelner septischer Kardiomyozyten experimentell untersucht mit der Hypothese, dass die *in vivo* gezeigte Aufhebung der kardialen Depression durch Katecholaminen auch auf einer Verbesserung der Verkürzung einzelner Kardiomyozyten beruht. Es wurden Kardiomyozyten aus dem Arbeitsmyokard von C57BL/6 Mäusen durch die Langendorff-Perfusionstechnik isoliert. Danach wurde eine Gruppe der Zellen in Kulturmedium mit Lipopolysaccharid (LPS) sechs Stunden lang inkubiert, um eine bakterielle Sepsis zu simulieren. Die zweite Gruppe wurde in Kulturmedium ohne LPS sechs Stunden lang inkubiert. Anschließend wurden beide Gruppen in verschiedenen Frequenzen elektrisch stimuliert. Die Stimulation erfolgte jeweils mit oder ohne Perfusion von Orciprenalin, ein nicht-selektives  $\beta$ -Sympathomimetikum, um die Katecholamintherapie in einer septischen Kardiomyopathie zu simulieren. Die Sarkomerverkürzung der jeweiligen Zellen wurde lichtmikroskopisch registriert. Daraus wurden die folgenden Parameter numerisch erfasst: Ruhesarkomerlänge, Verkürzungsamplitude, Verkürzungsgeschwindigkeit und Relaxationsgeschwindigkeit.

Durch diese Studie konnte zunächst die depressive Wirkung von LPS auf die Sarkomerverkürzung demonstriert werden, analog zu den vorherigen Ergebnissen unserer Arbeitsgruppe. Des Weiteren konnte gezeigt werden, dass diese Beeinträchtigung der Sarkomerverkürzung unter Einsatz von Orciprenalin nicht nur teilweise aufgehoben, sondern sogar überkompensiert wird. Damit konnte der „Rettungseffekt“ einer Katecholamintherapie in einer septischen Kardiomyopathie vermittelt durch die  $\beta$ -Stimulation demonstriert werden. Es konnte somit die o.g. Hypothese bestätigt werden.

## 6 References

ACCP/SCCM Consensus Conference Committee. Definition for sepsis and organ failure and guidelines for the use of innovative therapies in sepsis. *Crit Care Med* 1992;864-874

Alexander C, Rietschel ET. Bacterial lipopolysaccharides and innate immunity. *J Endotoxin Res* 2001; 7: 167-202

Avlas O, Fallach R, Shainberg A, Porat E, Hochhauser E. Toll-like receptor 4 stimulation initiates an inflammatory response that decreases cardiomyocyte contractility. *Antioxid Redox Signal* 2011; 15: 1895-1909

Barcroft H, Konzett H. Action of noradrenaline and adrenaline on human heart-rate. *Lancet*. 1949; 1: 147

Baumgarten G, Knuefermann P, Schuhmacher G, Vervolgyi V, von Rappard J, Dreiner U, Fink K, Djoufack C, Hoeft A, Grohe C, Knowlton AA, Meyer R. Toll-like receptor 4, nitric oxide, and myocardial depression in endotoxemia. *Shock* 2006; 25: 43-49

Bone RC. Toward an epidemiology and natural history of SIRS (Systemic inflammatory response syndrome). *JAMA* 1992; 24: 3252-3455

Boyd JH, Mathur S, Wang Y, Bateman RM, Walley KR. Toll-like receptor stimulation in cardiomyocytes decreases contractility and initiates an NF- $\kappa$ B dependent inflammatory response. *Cardiovasc Res* 2006; 72: 384-393

Buer J and Balling R. Mice, microbes and models of infection. *Nat Rev Genet*. 2003; 4: 195-205 (Online image) Retrieved October 18, 2015 from [http://www.nature.com/nrg/journal/v4/n3/fig\\_tab/nrg1019\\_F1.html](http://www.nature.com/nrg/journal/v4/n3/fig_tab/nrg1019_F1.html)

Charpentier J, Luyt CE, Fulla Y, Vinsonneau C, Cariou A, Grabar S, Dhainaut JF, Mira JP, Chiche JD. Brain natriuretic peptide: a marker of myocardial dysfunction and prognosis during severe sepsis. *Crit Care Med* 2004; 32: 660-665

Clark WA, Decker ML, Behnke-Barklay M, Janes DM, Decker RS. Cell contact as an independent factor modulating cardiac myocyte hypertrophy and survival in long-term primary culture. *J Mol Cell Cardiol* 1998; 30: 139-155

Cohen J. Sepsis and septic shock: inching forwards. *Clin Med*. 2009; 9: 256-257

Conly J, Johnston B. Where are all the new antibiotics? The new antibiotic paradox. *Can J Infect Dis Med Microbiol* 2005; 16: 159-160

Craig R, Lee KH, Mun JY, Torre I, Luther PK. Structure, sarcomeric organization, and thin filament binding of cardiac myosin-binding protein-C. *Pflugers Arch* 2014; 466: 425-31

Ehrentraut S, Lohner R, Schwederski M, Ehrentraut H, Boehm O, Noga S, Langhoff P, Baumgarten G, Meyer R, Knuefermann P. In vivo Toll-like receptor 4 antagonism restores cardiac function during endotoxemia. *Shock* 2011; 36: 613 - 620

Fernandes CJ Jr, Akamine N, Knobel E. Myocardial depression in sepsis. *Shock* 2008; Suppl 1: 14-17

Ferrero E, Jiao D, Tsuberi BZ, Tesio L, Rong GW, Haziot A, Goyert SM. Transgenic mice expressing human CD14 are hypersensitive to lipopolysaccharide. *Proc Natl Acad Sci* 1993; 90: 2380-2384

Franke WW, Borrmann CM, Grund C, Pieperhoff. The area composita of adhering junctions connecting heart muscle cells of vertebrates. I. Molecular definition in intercalated disks of cardiomyocytes by immunoelectron microscopy of desmosomal proteins. *Eur J Cell Biol* 2006; 85:69-82

Freedman NJ, Liggett SB, Drachman DE, Pei G, Caron MG, Lefkowitz RJ. Phosphorylation and desensitization of the human  $\beta_1$ -adrenergic receptor, involvement of G protein-coupled receptor kinases and cAMP-dependent protein kinase. *J Biol Chem* 1995; 270: 17953–17961

Godowski PJ. A smooth operator for LPS responses. *Nat Immunol*. 2005; 6: 544-546

Haziot A, Lin XY, Zhang F, Goyert SM. The induction of acute phase proteins by lipopolysaccharide uses a novel pathway that is CD14-independent. *J Immunol*. 1998; 160: 2570-2572

He Q, Spiro MJ. Suspension culture of differentiated rat heart myocytes on non-adhesive surfaces. *J Mol Cell cardiol* 1996; 28: 1177-1186

Honerjäger, P. Pharmacology of positive inotropic phosphodiesterase III inhibitors. *Eur Heart J* 1989; 10: 25-31

Jiang W, Sun R, Wei H, Tian Z. Toll-like receptor 3 ligand attenuates LPS-induced liver injury by down-regulation of toll-like receptor 4 expression on macrophages. *Proc Natl Acad Sci* 2005; 102: 17077-17082

Jones GR, Lowes JA. The systemic inflammatory response syndrome as a predictor of bacteraemia and outcome from sepsis. *QJM* 1996; 89: 515-22

Kapadia S, Lee J, Torre-Amione G, Birdsall HH, Ma TS, Mann DL. Tumor necrosis factor- $\alpha$  gene and protein expression in adult feline myocardium after endotoxin administration. *J Clin Invest*. 1995; 96:1042-1052

Kempelmann HJ. Der Einfluss von Gelsolin auf die Verkürzung isolierter ventrikulärer Kardiomyozyten der Maus. 2005; Diss Med Fak Universität Bonn

Kinugawa KI, Kohmoto O, Yao A, Serizawa T, Takahashi T. Cardiac inducible nitric oxide synthase negatively modulates myocardial function in cultured rat myocytes. *Am J Physiol.* 1997; 272:35-47

Kohl P, Camelliti P, Burton FL, Smith GL. Electrical coupling of fibroblasts and myocytes: relevance for cardiac propagation. *J Electrocardiol* 2005; 38: 45-50

Knuefermann P, Schwederski M, Velten M, Krings P, Stapel H, Rudiger M, Boehm O, Fink K, Dreiner U, Grohe C, Hoeft A, Baumgarten G, Koch A, Zacharowski K, Meyer R. Bacterial DNA induces myocardial inflammation and reduces cardiomyocyte contractility: role of toll-like receptor 9. *Cardiovasc Res* 2008; 78: 26-35

Kreyman G, Wolf M. Geschichte und Definition der Sepsis - Brauchen wir eine neue Terminologie? *Anesthesiol Intensivmed Notfallmed Schmerzther* 1996; 31: 9-14

Lakhani SA, Bogue CW. Toll-like-receptor signalling in sepsis. *Curr Opin Pediatr* 2003; 15: 278-282

Levy MM, Fink MP, Marshall JC, Abraham E, Angus D, Cook D, Cohen J, Opal SM, Vincent JL, Ramsay G, International Sepsis Definitions Conference. 2001 SCCM/ESICM/ ACCP/ATS/SIS International Sepsis Definitions Conference. *Intensive Care Med.* 2003; 29: 530-538

Lien E, Means TK, Heine H, Yoshimura A, Kusumoto S, Fukase K, Fenton MJ, Oikawa M, Qureshi N, Monks B, Finberg RW, Ingalls RR, Golenbock DT. Toll-like receptor 4 imparts ligand-specific recognition of bacterial lipopolysaccharide. *J Clin Invest* 2000; 105: 497-504

Linz KW, Meyer R. Profile and kinetics of L-type calcium current during the cardiac ventricular action potential compared in guinea-pigs, rats and rabbits. *Pflügers Arch* 2000; 439: 588-599

Lohner R, Schwederski M, Narath C, Klein J, Duerr GD, Torno A, Knuefermann P, Hoeff A, Baumgarten G, Meyer R, Boehm O. Toll-like receptor 9 promotes cardiac inflammation and heart failure during polymicrobial sepsis. *Mediators Inflamm* 2013; 10: 1155-1168

Mann DL. Innate immunity and the failing heart: the cytokine hypothesis revisited. *Circ Res*. 2015; 116: 1254-1268

Martin GS, Mannino DM, Eaton S, Moss M. The epidemiology of sepsis in the United States from 1979 through 2000. *N Engl J Med* 2003; 348: 1546-1554

Massion PB, Balligand JL. Modulation of cardiac contraction, relaxation and rate by the endothelial nitric oxide synthase (eNOS): lessons from genetically modified mice. *J Physiol*. 2003; 546: 63-75

Medzhitov R, Janeway C Jr. The Toll receptor family and microbial recognition. *Trends Microbiol*. 2000; 10: 452-456

Medzhitov R. Toll-Like receptors and innate immunity. *Nat Rev Immunol*. 2001; 1: 135-145

Meyer R. Oberflächenstruktur, Membranströme und Kontraktilität isolierter Herzmuskelzellen. Habilitationsschrift Med Fak Universität Bonn 1989

Mukhopadhyay S, Herre J, Brown GD, Gordon S. The potential for toll-like receptors collaborate with other innate immune receptors. *Immunology* 2004; 112: 521-530

Muller-Werdan U, Buerke M, Ebel H, Heinroth KM, Herklotz A, Loppnow H, Russ M, Schlegel F, Schlitt A, Schmidt HB, Soeffker G, Werdan K. Septic cardiomyopathy – A not yet discovered cardiomyopathy? *Exp Clin Cardiol* 2006; 11: 226-236

Nagai Y, Akashi S, Nagafuku M, Ogata M, Iwakura Y, Akira S, Kitamura T, Kosugi A, Kimoto M, Miyake K. Essential role of MD-2 in LPS responsiveness and TLR4 distribution. *Nat Immunol* 2002; 3: 667-72

Oliveira LS, de Queiroz NMGP, Veloso LVS. A defective TLR4 signaling for IFN- $\beta$  expression is responsible for the innately lower ability of BALB/c macrophages to produce NO in response to LPS as compared to C57BL/6. *PLoS ONE* 2014; 9: 10-13

Pagani FD, Baker LS, His C, Knox M, Fink MP, Visner MS. Left ventricular systolic and diastolic dysfunction after infusion of tumor necrosis factor- $\alpha$  in conscious dogs. *J Clin Invest* 1992; 90: 389-398

Pålsson-McDermott EM and O'Neill LAJ. Signal transduction by the lipopolysaccharide receptor, Toll-like receptor-4. *Immunology* 2004; 113: 153-162

Parrillo JE, Parker MM, Natanson C, Suffredini AF, Danner RL, Cunnion RE, Ognibene FP. Septic shock in humans. Advances in the understanding of pathogenesis, cardiovascular dysfunction and therapy. *Ann Intern Med* 1990; 113: 227-242

Pasteur L. Mémoire sur la fermentation appelée lactique, *Comptes rendus des seances de l'Academie des Sciences* 1857; 45: 913-916

Ramirez P, Villarreal E, Gordon M, Gómez MD, de Hevia L, Vacacela K, Gisbert T, Quinzá A, Ruiz J, Alonso R, Bonastre J, Vila J. Septic participation in cardiogenic shock: exposure to bacterial endotoxin. *Shock* 2017; 47: 588-592

Rastaldo R, Pagliaro P, Cappello S, Penna C, Mancardi D, Westerhof N, Losano G. Nitric oxide and cardiac function. *Life Sci* 2007; 81: 779-793

Rensing H. Endotoxin. Pathogenetische Bedeutung bei der Sepsis. *Anaesthesist* 2003; 52: 7-13



Rittirsch D, Flierl MA, Ward PA. Harmful molecular mechanisms in sepsis. *Nat Rev Immunol* 2008; 8: 776–787

Ruiz N, Kahne D, Silhavy J. Transport of lipopolysaccharide across the cell envelope: the long road of discovery. *Nature Reviews Microbiol* 2009; 7: 677-683

Santos JL1, Andrade AA, Dias AA, Bonjardim CA, Reis LF, Teixeira SM, Horta MF. Differential sensitivity of C57BL/6 (M-1) and BALB/c (M-2) macrophages to the stimuli of IFN- $\gamma$ /LPS for the production of NO: correlation with iNOS mRNA and protein expression. *J Interferon Cytokine Res* 2006; 26: 682-688

Schletter J, Brade H, Brade L, Krüger C, Loppnow H, Kusumoto S, Rietschel ET, Flad HD, Ulmer AJ. Binding of lipopolysaccharide (LPS) to an 80-kilodalton membrane protein of human cells is mediated by soluble CD14 and LPS-binding protein. *Infect Immun* 1995; 63: 2576-2580

Schromm AB, Lien E, Henneke P, Chow JC, Yoshimura A, Heine H, Latz E, Monks BG, Schwartz DA, Miyake K, Golenbock DT. Molecular genetic analysis of an endotoxin nonresponder mutant cell line: a point mutation in a conserved region of MD-2 abolishes endotoxin-induced signaling. *J Exp Med* 2001; 194: 79-88

Schumacher G. TLR-4-Rezeptor-vermittelter Einfluss von Endotoxin auf die Kontraktilität isolierter Kardiomyozyten der Maus. 2006; Diss Med Fak Universität Bonn

Schumann RR, Leong SR, Flagg GW, Gray PW, Wright SD, Mathison JC, Tobias PS, Ulevitch RJ. Structure and function of lipopolysaccharide binding protein. *Science* 1990; 249: 1429-1431

Schuster, HP, Müller-Werdan U. (2000). *Intensivtherapie bei Sepsis und Multiorganversagen*. Berlin Heidelberg New York: Springer

Semmelweis IP. (1861). Die Ätiologie, der Begriff und die Prophylaxe des Kindbettfiebers. Wien: Pest

Shanks RG, Brick I, Hutchison K, Roddie IC. Stimulation of adrenergic beta-receptors by orciprenaline. Br Med J 1967; 1:610-612

Shear MJ, Turner FC, Perrault A, Shovelton T. Chemical treatment of tumors. V. Isolation of the hemorrhage-producing fraction from *Serratia marcescens* (*Bacillus prodigiosus*) culture filtrate. J Natl Cancer Inst 1943; 81-97

Tiemann K, Weyer D, Djoufack PC, Ghanem A, Lewalter T, Dreiner U, Meyer R, Grohe C, Fink KB. Increasing myocardial contraction and blood pressure in C57BL/6 mice during early postnatal development. Am J Physiol 2003; 284: H464-H474

Ullrich R., Scherrer-Crosbie M., Bloch KD, Ichinose F., Nakajima H., Picards MH. Congenital deficiency of nitric oxide synthase 2 protects against endotoxin-induced myocardial dysfunction in mice. Circulation 2000; 102: 1440-1446

Vervölgyi V. Die Wirkung der bakteriellen Sepsis auf die elektromechanische Kopplung und die Hypertrophieentwicklung des Herzens. 2007; Inaugural-Dissertation Vet.-Med Fak Universität Gießen

Visintin M, Settanni G, Maritan A, Graziosi S, Marks JD, Cattaneo A. The intracellular antibody capture technology (IACT): towards a consensus sequence for intracellular antibodies. J Mol Biol 2002; 317: 73-83

Wagner DR, McTiernan C, Sanders VJ, Feldman AM. Adenosine inhibits lipopolysaccharide-induced secretion of tumor necrosis factor- $\alpha$  in the failing human heart. Circulation 1998; 97: 521-524

Warner SJ, Mitchell D, Savage N, McClain E. Dose-dependent reduction of lipopolysaccharide pyrogenicity by polymyxin B. *Biochem Pharmacol* 1985; 34: 3995-3998

Weisser-Thomas J, Kempelmann H, Nickenig G, Grohé C, Fink K, Meyer R. Influence of gelsolin deficiency on excitation contraction coupling in adult murine cardiomyocytes. *J Physiol Pharmacol* 2015; 66, 373-383

## 7 Supplement: Tables of Measured Parameters

### 7.1 Legend

Hz	Stimulation Frequency
Mean	Mean
SD	Standard Deviation
n	number of cells tested
Tyrode	Tyrode group
Tyrode + Orci	Tyrode group with orciprenaline
CM	incubated group
CM + Orci	incubated group with orciprenaline
CM + LPS	with LPS incubated group
CM + LPS + Orci	with LPS incubated group with orciprenaline

## 7.2 Resting Sarcomere Length

HZ	Tyrode + Orcki			Tyrode			CM		
	Mean	SD	N	Mean	SD	N	Mean	SD	N
0.5	1.837696	0.04175956	46	1.8544	0.04270906	45	1.826435	0.04109283	23
1	1.840273	0.0400792	44	1.858174	0.03643765	46	1.82555	0.04084051	20
2	1.836913	0.04007483	46	1.848191	0.03961809	47	1.823635	0.04273981	23
4	1.835163	0.03883845	43	1.84915	0.03561946	40	1.820709	0.04715719	22
6	1.827537	0.0390289	41	1.839	0.04274843	43	1.818455	0.05187597	22
8	1.829571	0.03882678	42	1.83931	0.03687255	42	1.821039	0.04634041	26
10	1.82225	0.0397426	40	1.836774	0.04330028	31	1.81044	0.04199472	25

HZ	CM + Orcki			CM + LPS + Orcki			CM + LPS		
	Mean	SD	N	Mean	SD	N	Mean	SD	N
0.5	1.77825	0.04850626	22	1.76725	0.0498202	24	1.791778	0.04123874	18
1	1.782349	0.04296523	16	1.776654	0.06135663	26	1.790333	0.03447089	12
2	1.776902	0.03255201	17	1.777182	0.04396326	22	1.792867	0.04470247	15
4	1.779823	0.050023	19	1.777727	0.04382654	22	1.805143	0.04996746	14
6	1.762039	0.042319	15	1.77081	0.03315031	21	1.796818	0.07076414	11
8	1.770139	0.032378	18	1.770875	0.03394584	24	1.792692	0.05278634	13
10	1.760283	0.068239	21	1.767789	0.05526491	19	1.781533	0.03378856	15

## 7.3 Shortening Amplitude

HZ	Tyrode + Orchi			Tyrode			CM		
	Mean	SD	N	Mean	SD	N	Mean	SD	N
0.5	0.1523617	0.03896736	47	0.1091111	0.04324677	45	0.06421739	0.04709575	23
1	0.1242222	0.04525391	45	0.07491304	0.02783269	46	0.0448125	0.0343981	16
2	0.1113617	0.04133116	47	0.0606383	0.02407274	47	0.04952941	0.04421979	17
4	0.1187045	0.04936272	44	0.0707	0.03482204	40	0.05205263	0.04223805	19
6	0.1637317	0.06575828	42	0.1157674	0.05664671	43	0.07026667	0.04178069	15
8	0.1787381	0.02283997	43	0.1128974	0.04402977	39	0.083	0.04432572	14
10	0.166625	0.03309687	41	0.1095667	0.04755373	30	0.07157143	0.04289356	21

HZ	CM + Orchi			CM + LPS + Orchi			CM + LPS		
	Mean	SD	N	Mean	SD	N	Mean	SD	N
0.5	0.1211304	0.04817327	23	0.12448	0.04904129	25	0.0598	0.04882795	20
1	0.10455	0.04114988	20	0.1150769	0.0579363	26	0.04461538	0.02899293	13
2	0.09869565	0.04653878	23	0.0945	0.03228564	22	0.03473333	0.02781178	15
4	0.109	0.0437286	22	0.08340909	0.04000249	22	0.03942857	0.02156106	14
6	0.1466818	0.07148452	22	0.119619	0.03687202	21	0.03981818	0.03678703	11
8	0.1444615	0.03462397	26	0.1295	0.09776636	24	0.0458125	0.06124946	16
10	0.13296	0.04938047	25	0.1092	0.04405064	20	0.06564286	0.0346246	15

## 7.4 Shortening Speed

HZ	Tyrode + Orchi			Tyrode			CM		
	Mean	SD	N	Mean	SD	N	Mean	SD	N
0.5	7.605298	3.038752	47	5.794533	2.677847	45	4.468136	2.277331	22
1	6.7098	2.908099	45	4.522109	2.188971	46	3.43025	1.791918	16
2	6.564511	2.988965	47	3.895319	1.388623	47	3.141471	2.806596	17
4	7.570273	3.008582	44	4.122225	1.895514	40	3.080158	2.416993	19
6	7.84381	3.286478	42	4.743046	2.365062	43	3.679	2.688332	15
8	7.860465	3.568208	43	4.582857	2.316087	42	3.699375	1.554957	16
10	7.240415	3.491793	41	4.412871	2.314439	31	3.543667	1.652339	21

HZ	CM + Orchi			CM + LPS + Orchi			CM + LPS		
	Mean	SD	N	Mean	SD	N	Mean	SD	N
0.5	7.136435	2.880142	23	5.94588	3.209838	25	2.58145	2.443199	20
1	6.2256	2.754199	20	5.379231	2.58942	26	2.353	1.220107	13
2	5.544391	2.500017	23	4.804636	2.375489	22	2.3094	1.35034	15
4	6.4395	2.592926	22	5.013091	2.011922	22	2.259072	1.335056	14
6	6.938727	2.103701	22	5.330857	2.766795	21	2.370417	1.232327	12
8	6.752269	2.21494	26	5.286708	2.25204	24	2.5014	1.834629	15
10	6.2604	2.584746	2	4.94065	1.90705	20	2.379357	1.205238	15

## 7.5 Relaxation Speed

HZ	Tyrode + Orchi			Tyrode			CM		
	Mean	SD	N	Mean	SD	N	Mean	SD	N
0.5	5.80517	2.957723	47	3.884822	2.162217	45	2.516	1.262093	20
1	4.826622	2.573603	45	2.72337	1.671507	46	1.789	1.397317	16
2	4.528979	2.581084	47	2.024542	1.202826	48	1.670812	1.440541	16
4	5.236591	2.603436	44	2.5171	1.538392	40	2.004684	1.932093	19
6	5.620572	2.811966	42	3.275837	2.028436	43	2.1864	2.453117	15
8	5.850395	2.993081	43	3.117	1.949845	42	1.905333	1.684684	18
10	5.359366	2.930547	41	3.009452	1.84792	31	1.891571	1.456189	21

HZ	CM + Orchi			CM + LPS + Orchi			CM + LPS		
	Mean	SD	N	Mean	SD	N	Mean	SD	N
0.5	5.405826	2.967989	23	4.51236	3.137887	25	2.136	2.123577	20
1	4.89785	2.595334	20	3.970923	2.824979	26	1.337923	0.9088844	13
2	4.811565	2.815322	23	3.637136	2.797671	22	1.078133	0.8161232	15
4	5.265954	2.703801	22	3.649409	3.061155	22	1.375929	0.9373624	14
6	6.040773	3.671307	22	3.991333	2.923011	21	1.406455	0.8109108	11
8	5.783154	3.537346	26	3.864875	3.117442	24	1.798625	1.567051	16
10	5.11532	3.129091	25	3.6113	2.574592	20	1.556571	0.8885186	15



## **8 Acknowledgements**

I would like to thank my lovely wife, Woo Youn Kwon, and my kids, Un and Heon for their enduring support. Without them I would not be the person that I am today. I want to thank my parents for my body and brain, which is the basis of my intellect and humor. I want to thank them for making me a Korean. I am enjoying it a lot. I want to thank my parents-in-law, Mr. Eue-Chan Kwon and Mrs. Moon-Oog Lee, for trusting me with their daughter, their center of life, and keeping on believing in me. Without their daughter, I would have been lost.

I thank my boss and teacher Professor Dr. med. Thorsten Wahlers, who taught me what it means to deliver rigorously and painstakingly the best medical care for my patients. I thank Professor Dr. med. Yeong-Hoon Choi, who proof-read this work multiple times and helped me and encouraged me not to give up. I also thank Professor Dr. med. Khosro Hekmat who cares for me and teaches me the ways of a calm and competent surgeon without compromise. I thank my good friends and colleagues Ilija Djordjevic, Fabian Dörr, Orhan Özel and many others who care for me and help me with critics and praises. I want to thank all my friends at the Hanbit Korean Church in Cologne for believing in me and helping me to stay focused.

I want to thank Professor Dr. rer. nat. Rainer Meyer, my doctoral “father” and an inspiring example, with the best of my heart. He picked me up from despair and got me back on the right track multiple times. He has not only helped me through my academic carrier, but has also encouraged me to look above and become an active part of this beautiful, patient and rewarding country of Germany, in which I am a proud and passionate part of. Without him and his enduring support, this work would have been not possible at all.

Lastly, but mostly, I want to thank my Lord and Savior, Jesus Christ of Nazareth, who gave His life for me. I thank Him for being with me day by day and teaching me that in the moments when I am weak, I can truly be strong with His power.